The coordination chemistry of 2-pyridone and its derivatives

Jeremy M. Rawson and Richard E.P. Winpenny
Department of Chemistry, The University of Edinburgh, West Mains Road, Edinburgh EH9 3JJ (UK)

(Received 22 March 1994)

CONTENTS

Correspondence to: R.E.P. Winpenny, Department of Chemistry, The University of Edinburgh, West Mains Road, Edinburgh, EH9 3JJ, UK.

0010-8545/95/$29.00
SSDI 0010-8545(94)01117-T

© 1995 – Elsevier Science S.A. All rights reserved.

ABSTRACT

This review covers the coordination chemistry of 2-pyridone (2-hydroxypyridine) and its derivatives from 1968 to 1993. The derivatives studied have chiefly been 2-pyridone itself and those substituted in the 6-position of the ring, in particular 6-methyl-2-pyridone and 6-chloro-2-pyridone. These ligands have found their major usage as 1,3-bridging ligands akin to carboxylates. A large number of dimeric complexes have been synthesized with elements including Cr, Mo, W, Tc, Re, Ru, Os, Rh, Ir, Pd, Pt and Cu, and in which the metal–metal bond order varies from four to zero. The structural chemistry of these dimeric complexes is discussed, as are physical studies designed to increase the understanding of metal–metal bonding. Larger polymetallic arrays can be made with first-row metals such as chromium, cobalt and copper. Work on platinum complexes of 2-pyridone has been important in modelling the interaction of *cis*-$[Pt(NH_3)_2Cl_2]$ with uracil nucleobases; this work is also reviewed. Dimeric rhodium(I) and iridium(I) complexes display interesting photochemistry, and this work is described. A recent development is the use of 2-pyridones as bridging ligands in heterometallic assemblies, especially of copper and lanthanoids and Group 2 metals.

1. INTRODUCTION

The anion of 2-pyridone (or 2-hydroxypyridine) and substituted derivatives thereof have found their chief use in coordination chemistry as 1,3-bridging ligands when they behave similarly to carboxylates. They have had an important role in the 30-year history of metal multiple bonds, e.g. they were present in the first multiple-bonded dimers of a complete triad of transition metals [1] and were used in the first complex to contain an Os–Os triple bond [2]. In addition, they have featured in a large number of other multiple-bonded metal dimers. Such ligands have also been used to model the binding of platinum to DNA and to characterize in more detail "platinum blues" [3]. Interesting polynuclear complexes of these ligands have also been reported, one of the largest being a dodecanuclear complex of cobalt [4]. More recently, the presence of two different donor atoms has led to the use of these ligands to synthesize heterometallic polynuclear arrays containing d- and f-block metals [5–8] and d- and s-block metals [8–10].

Although there has been extensive work in this area, there remain some curious omissions. Thus, for example, although the number of manganese and iron carboxylate arrays synthesized is legion [11–14], there are no reported, fully characterized polynuclear compounds of these elements with 2-pyridone-based ligands. Indeed, with the exception of chromium and copper, there is a paucity of structural informa-

tion on the complexes of first-row metals with these ligands. Furthermore, although many different derivatives of 2-pyridone can be readily synthesized, coordination chemists have tended to restrict their interest to only the parent ligand and to the 6-chloro and 6-methyl derivatives, despite the possibility that the steric and electronic properties of the ligand might be modified by more extensive substitution.

The aims of this review are therefore twofold: to assess what has been done and to highlight some of the gaps in the chemistry of these ligands.

2. SCOPE AND STRUCTURE OF REVIEW

This review is intended to cover all work done on 2-pyridone ligands up to the end of 1993, with later work of which we are aware included. We have not included work on 1-substituted 2-pyridones, nor work on other pyridone ligands, e.g. 4-pyridone, as the chemistry of such ligands is quite different. Other related ligands, e.g. 2-mercaptopyridine, have also been excluded.

The terminology used below is somewhat inexact, but we feel that this helps enormously in improving the digestibility of the review. Thus we always refer to these ligands as "pyridones" even when there is the possibility of the pyridinol tautomer being present. Secondly, we refer to "pyridone ligands" where the ligand is deprotonated, and "protonated pyridones" where the ligand is present as the neutral form. The context should make the species present clear. Referring incessantly to "pyridone anion ligands" or to "pyridinato" or "pyridonide" ligands was considered to be inelegant and wilfully obscure. A common system of abbreviations is also used whereby ligands are referred to as "xhp", where "hp" refers to the parent ligand and "x" to the nature of the substituent. If preceded by a number, the name refers to the position on the ring at which the substituent occurs, e.g. 3-mhp would refer to 3-methyl-2-pyridone. If no number is included, the substituent is in the 6-position, as is most commonly the case.

Only one complex of an early transition metal has been reported for these ligands. This is mentioned in Section 4. Thereafter the complexes are considered triad by triad. Relationships between similar complexes from different triads are discussed in the conclusion.

3. SYNTHESIS, STRUCTURES AND PROPERTIES OF 2-PYRIDONES

3.1. *Range of derivatives*

Several derivatives of 2-pyridone are commercially available or readily synthesized. A list of these derivatives is given in Table 1. The majority of coordination chemistry reported involves anions of either the parent ligand (Hhp) or derivatives substituted in the 6-position of the ring, in particular 6-methyl- and 6-chloro-2-pyridones (Hmhp and Hchp respectively). It is unclear why the range of ligands

TABLE 1
Availability of derivatives of 2-pyridone

Compound	Abbreviation	Synthesis	Reference
2-Pyridone	Hhp	Commercially available	—
6-Methyl-2-pyridone	Hmhp	Commercially available	
6-Chloro-2-pyridone	Hchp	Commercially available	
3-Cyano-2-pyridone	H(3-CN)hp	Commercially available	
3-Cyano-6-methyl-2-pyridone	H(3-CN)mhp	Commercially available	
4-Nitro-2-pyridone	H(4-NO_2)hp	Commercially available	
5-Chloro-2-pyridone	H(5-Cl)hp	Commercially available	
6-Bromo-2-pyridone	Hbhp	Base hydrolysis of 2,6-dibromopyridine	15
6-Amino-2-pyridone	Hahp	Acid hydrolysis of 2,6-diaminopyridine	16
3-Alkyl- or 4-alkyl-2-pyridone	H(3-R)hp	Acid hydrolysis of related amino derivative via diazonium salt	17
6-Fluoro-2-pyridone	Hfhp	No reported synthesis	—
4-*tert*-Butyl-2-pyridone	H(4-Bu)hp	Acid hydrolysis of 4-*tert*-butyl-2-aminopyridine via diazonium salt	18
6-Diphenylphosphino-2-pyridone	Hphp	Reaction of PPh_2Li with 2-chloro-6-methoxypyridine, followed by hydrolysis	19
3-Hydroxy-2-pyridone	H(3-OH)hp	Commercially available	

used has been so restricted. There are a few cases where pyridone ligands substituted in other positions have been used: e.g. copper complexes of a wide range of derivatives [20–22], some of which have been structurally characterized [20]; a report of the use of 2,3-dihydroxypyridine as a chelating agent for a variety of metals [23]; and the use of 4-*tert*-butyl-2-pyridone as a chelating ligand for molybdenum [18].

Those ligands which are not commercially available can be synthesized via a variety of routes which are also listed in Table 1. 6-Fluoro-2-pyridone, a ligand used in several fascinating papers from Cotton's research group, is not commercially available, nor has any synthesis of this ligand been published as far as we have been able to ascertain.

3.2. Tautomerism and physical properties

The tautomerism between neutral 2-pyridinols and 2-pyridones (Scheme 1) is one of the simplest examples of heterocyclic tautomerism and has been known since 1907 [24]. It has been extensively studied, and was authoritatively reviewed in 1963

Scheme 1. The tautomeric equilibrium in 2-pyridones.

and 1976 by Katritzky and others [25,26]. In the 18 years since the latter review appeared, work has continued and most physical techniques, including IR, multinuclear NMR, UV–visible and fluorescence spectroscopy, and X-ray crystallography, have been used to study this phenomenon, and a number of extended theoretical papers have addressed the issue [27,28]. It is beyond the scope of this article to review this material. The conclusions from these studies can be summarized as follows. In the gas phase, the stability of the two tautomers tends to be very similar, e.g. for Hhp the tautomerism energy is measured at 0.8 kcal mol^{-1}, with the hydroxy form being the more stable [29]. In solution, the polarity of the solvent is crucial, with polar solvents strongly favouring the pyridone form, while in non-polar solvents both tautomers can exist. In the solid state, the pyridone form is often favoured [30,31]; however, self-association into dimers is important.

Substituents affect the position of the tautomeric equilibrium, and for monosubstituted derivatives it has been shown that the strongest influence comes from substituents in the 6-position. The presence of electron-withdrawing groups, e.g. F, Cl or OCH_3, favours the pyridonal form. The reason for this is normally considered to be a change in the relative basicity of the nitrogen and oxygen atoms; the presence of the strongly electronegative group decreases the basicity of the nitrogen sufficiently such that the enol form predominates. Most other derivatives show a preference for the pyridone form. This has been shown very elegantly by X-ray crystallography on Hchp [32], H(5-Cl)hp [31], Hbhp [33] and a mixture of Hchp and Hhp [34]. For the pure compounds centrosymmetric hydrogen-bonded dimers result (Fig. 1; symbols used in the figures are defined in Exhibit 1). For Hchp and Hbhp, the hydrogen of the hydrogen bond lies nearer the oxygen. For H(5-Cl)hp, the hydrogen

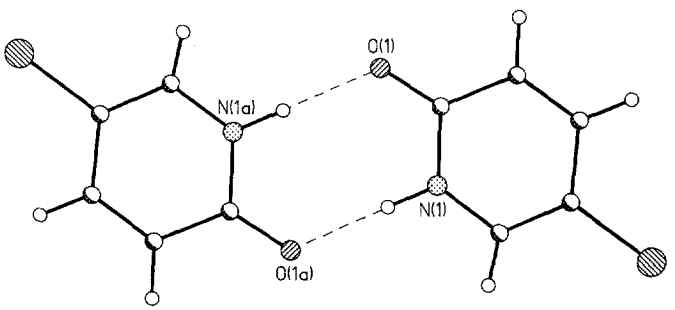

Fig. 1. The hydrogen-bonding interaction between two molecules of H(5-Cl)hp within the crystal (based on data from ref. 31).

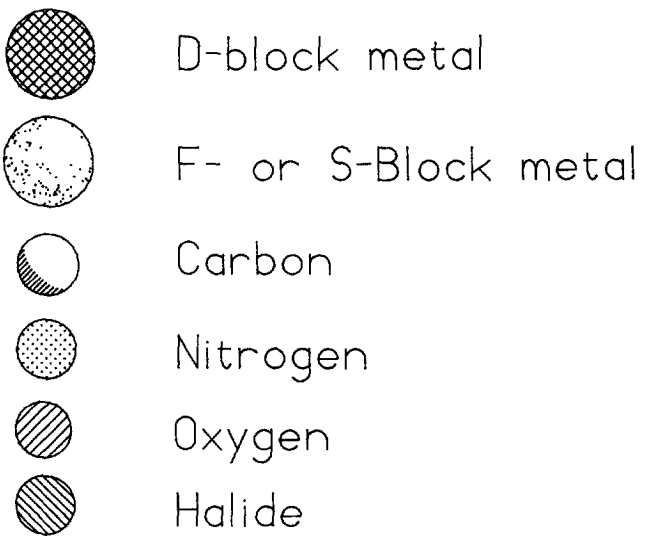

Exhibit 1. Definitions of symbols used in the figures.

lies nearer the nitrogen. In the mixed Hchp–Hhp dimer, the pair of hydrogen-bonded molecules lie "head-to-head" with H bonds between like atoms (Fig. 2), rather than between unlike atoms as in the pure phases. This allows the ionizable hydrogen of Hchp to lie on the oxygen, and that of Hhp to lie on the nitrogen, which suggests that the ligands are present as the -ol and -one forms respectively.

Less work has been carried out on the tautomerization of the deprotonated ligands. The presence of two tautomeric forms, which can be influenced by substituents, is potentially of importance in the coordination chemistry of these ligands. However, there are several examples where similar complexes of different derivatives have been synthesized, e.g. $M_2(xhp)_4$ (where M ≡ Cr, Mo, W or Rh and xhp ≡ mhp

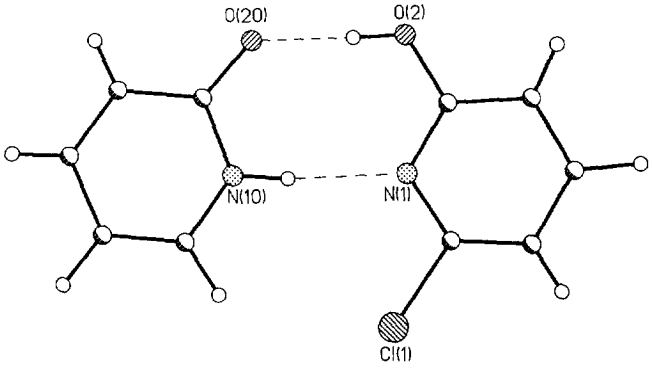

Fig. 2. The hydrogen-bonding interaction between molecules of Hchp and Hhp within the crystal (based on data from ref. 34).

or chp). There are a few examples of occasions where attempts to make similar complexes have led to different structures with the two ligands. It might also be expected that more polarizable second- and third-row metals might prefer binding to the nitrogen donor, and thus might alter the position of the tautomeric equilibrium. For example, Hhp binds to first-row metals through oxygen [35–37] but to platinum via the ring nitrogen [38].

The ionization constants, UV–visible and IR spectra of several pyridones were reported by Spinner and White [39], although curiously they neglected the 6-halo-substituted derivatives completely. The pK_a values indicate that the pyridones studied are slightly weaker acids than *o*- or *p*-chlorophenol. The electronic absorption spectra show two or three strong π–π^* transitions at high energy. More recently, the fluorescence spectra of several derivatives including Hhp, Hmhp and Hchp have been reported [40]. Additionally, ^{13}C, ^{1}H and ^{17}O NMR studies have been reported for some pyridone derivatives [41,42].

3.3. *Comparison between 2-pyridones and other bridging ligands*

The anions of 2-pyridones belong to the class of triatomic bridging ligands. Other examples are shown in Scheme 2. The chief difference between the pyridones and the most commonly used ligands, the carboxylates, is the presence of two different donor atoms. In this, 2-pyridones resemble ligands such as methylenethiophosphinate (MTP). Like carboxylates, pyridones are easily derivatized, and there-

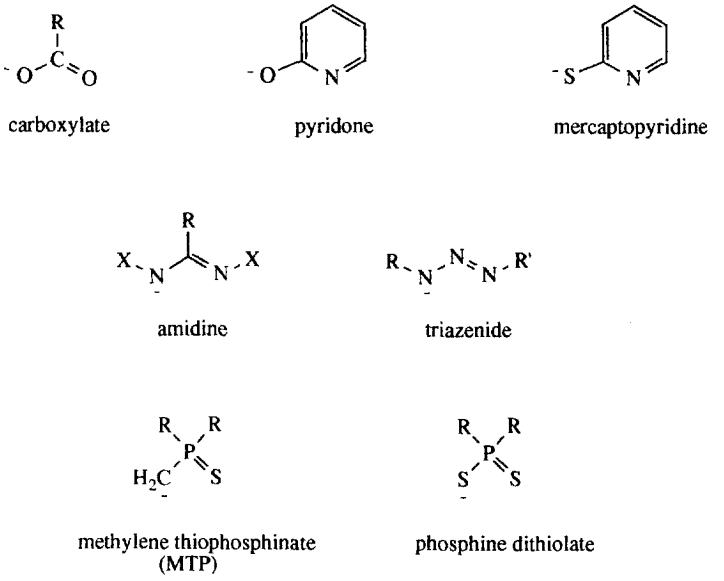

Scheme 2. Commonly used 1,3-bridging ligands.

fore some control of steric and electronic effects is, at least in theory, possible. This aspect of the ligand system has not been explored.

In pyridone ligands, one of the two donor atoms lies within a ring and this restricts the direction of the bonds from that atom, so that the angles at the nitrogen prefer to be close to 120° and the metal atom to which the nitrogen is bound is within the plane of the ring. This means that the number of bonding modes of 2-pyridones is more restricted than for carboxylates, and they rarely act as chelating ligands. Carboxylates can also act as multinucleating ligands — potentially each oxygen can bind to three different metals. Pyridones are again less flexible, and while they could potentially be tetranucleating — with the exocyclic oxygen bound to three metals and the nitrogen to a further metal — this bonding mode has not been observed. Trinucleating pyridones are, however, well known. The known bonding modes of pyridones are shown in Scheme 3.

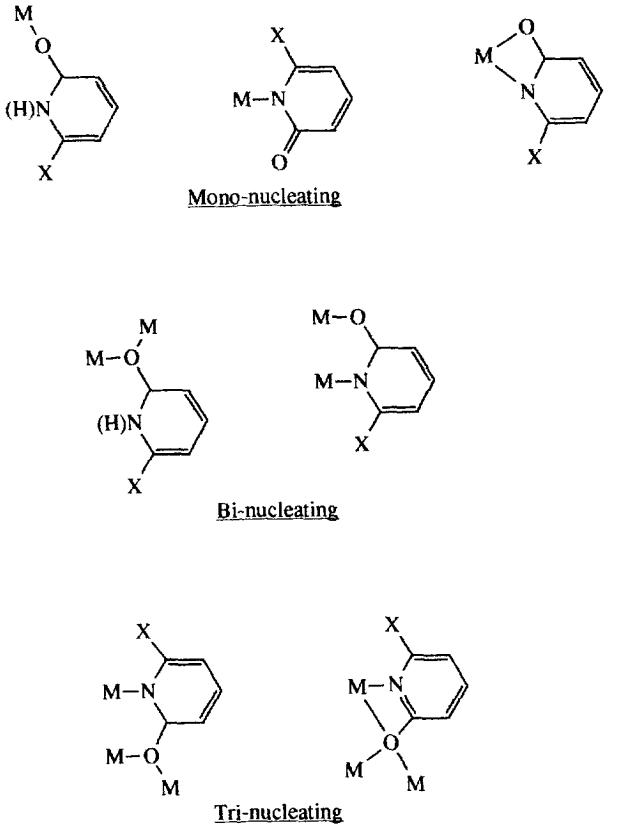

Scheme 3. Possible bonding modes for pyridone derivatives.

3.4. Complexes of protonated pyridone ligands

The earliest coordination chemistry reported for these ligands was an examination of the rate of linkage isomerism from the N-bound ligand to the O-bound ligand when attached to $[Co(NH_3)_5]^{3+}$ [43,44]. Shortly afterwards Reedijk [45,46] examined the binding of the protonated parent ligand, Hhp, to a series of transition metal ions, and from IR data concluded that Hhp is bound through the exocyclic oxygen to the metals. X-Ray structural analyses of $[Cu(Hhp)_6][NO_3]_2$ [35], $[Fe(Hhp)_6][NO_3]_3$ [36], $[Fe(Hmhp)_6][NO_3]_3$ [37] and $[Co(mhp)_4(NO_3)_2]$ [37] have confirmed this prediction. The binding of the ligands in these mononuclear species is in no way unusual, with the metal–oxygen bond lengths similar to those in other metal complexes of ketones [47]. More recently, a thorium complex, $[Th(Hhp)_6(NO_3)_2][NO_3]_2$ of the protonated ligand has been reported [48], which again features the ligand bound through the O donor. In all these crystallographically characterized complexes, the proton attached to the ring nitrogen atom is involved in hydrogen bonding, which may be intramolecular [37] or intermolecular [36].

4. COMPLEXES OF THE EARLY TRANSITION METALS

The only reported pyridone complex of a metal from Groups 3, 4 or 5 is the dinuclear vanadium complex $[V_2O_2Cl_4(Hmhp)_3]$ [49], prepared via air oxidation of $VCl_3.3THF$ (THF, tetrahydrofuran) in the presence of Hmhp under anhydrous conditions. The compound was isolated as bright blue crystals and consists of two face-sharing, distorted octahedral VO_4Cl_2 centres (Fig. 3). Two μ_2-pyridone oxygens are asymmetrically shared by the two V^{4+} centres with short contacts of 2.016(2)

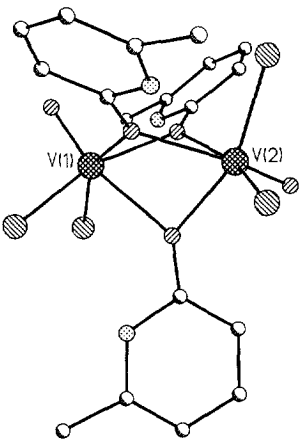

Fig. 3. The structure of $[V_2O_2Cl_4(Hmhp)_3]$ in the crystal (based on data from ref. 49).

and 2.043(2) Å and long contacts of 2.345(2) and 2.373(2) Å; the third pyridone oxygen is symmetrically bridging with a V–O distance of 2.096(2) Å. The V–V distance is quite large (3.175(1) Å), but still allows some sort of magnetic exchange interaction between the vanadium centres, which leads to a broadening of the hyperfine structure in the electron paramagnetic resonance (EPR) spectrum. The protonated nitrogen atoms take part in intermolecular hydrogen bonding with Cl atoms of neighbouring molecules.

5. THE CHROMIUM TRIAD

5.1. *Synthesis of dimeric Cr, Mo and W complexes*

The first reported pyridone complexes of the chromium triad were the dimers of formula $[M_2(mhp)_4]$ (M ≡ Cr, Mo, W), synthesized in 1978 by Cotton et al. [1]. Their unprecedented thermal and chemical stability in comparison with other multiple-bonded compounds and, in particular, the existence of isostructural complexes of all three metals of the triad have led to an extensive investigation of their chemistries especially the nature of the bonding between the metal atoms. Moreover, the properties observed in these compounds have led to the development of pyridone coordination chemistry in other triads.

Subsequent to the preparation of $[M_2(mhp)_4]$ complexes, $[M_2(chp)_4]$, $[M_2(fhp)_4(THF)]$ and, more recently, $[Mo_2(php)_4]$ have been prepared in an analogous fashion [50–52). In the case where M ≡ Cr or Mo, synthesis was achieved via ligand exchange with the dimeric metal acetates and the sodium [1,50,52] or lithium [51] salt of the pyridone anion, e.g.

$$4Na(mhp) + Cr_2(OAc)_4.2H_2O \rightarrow Cr_2(mhp)_4.H_2O + 4NaOAc + H_2O$$

The isolation of $[Cr_2(mhp)_4].H_2O$ is indicative of the hydrolytic stability of these compounds, although oxidative hydrolysis of these dimers can occur (see Section 5.4). This route is convenient for the preparation of these compounds, but it has been observed [53] to give products which contain up to 18% acetate. Whether this is in the form of $[M_2(mhp)_3(OAc)]$ as proposed in ref. 53, or the reported $[M_2(mhp)_2(OAc)_2]$ [54], or possibly some higher nuclearity pyridone–acetate oligomer as found for cobalt [4] or copper [55] is unclear. The reaction of lithium, sodium or silver salts of these ligands with metal acetates or chlorides has remained the predominant preparative route to pyridone complexes for all transition metals (see the following sections).

Complexes with the general formula $[M_2(xhp)_4]$ can also be prepared by reaction of $M(CO)_6$ (M ≡ Cr, Mo, W) with the protonated ligand in refluxing diglyme with near-quantitative (more than 95% recovered) yields [1,50]. The order of reactiv-

ity was found to be $W(CO)_6 > Mo(CO)_6 > Cr(CO)_6$. $[M_2(xhp)_4]$ complexes can be purified by sublimation typically at temperatures in excess of 200°C and 10^{-6} Torr [53].

Only partial substitution of NMe_2^- and O^iPr^- ligands occurs for the related Mo(III) complexes. Thus reaction of $[Mo_2(NMe_2)_6]$ or $[Mo_2(O^iPr)_6]$ with Hmhp gives $[Mo_2(NMe_2)_4(mhp)_2]$ and $[Mo_2(O^iPr)_4(mhp)_2]$ respectively [56,57]. Further addition of Hmhp gives the somewhat insoluble $[Mo_2(mhp)_4(NMe_2)_2]$ complex [56]. Incomplete substitution of Cl^- occurs when Hmhp reacts with $[Mo_2Cl_4(PEt_3)_4]$ yielding $[Mo_2(mhp)_2Cl_2(PEt_3)_2]$ [58]; however, Cl^- can be displaced by the use of the sodium salt of the pyridone ligand, e.g. $CrCl_2$ reacts with Na(mhp) to form $[Cr_2(mhp)_4]$ [53] and WCl_2 (prepared in situ by reduction of WCl_4 with sodium amalgam) reacts with Na(fhp) to give good yields of $[W_2(fhp)_4]$ [51]. These latter processes are driven by the insolubility of NaCl in the organic solvents used for the reactions. Thus the organometallic salt $[Cp_2Mo(hp)][PF_6]$ (Cp, cyclopentadienyl) was prepared by substitution of halide on $[CpMoX_2]$ by Na(hp) in the presence of $TlPF_6$ [59].

5.2. *Structures*

The structures of $[M_2(mhp)_4]$ and $[M_2(chp)_4]$ ($M \equiv Cr$, Mo, W) have been determined at several temperatures and as a variety of solvates [1,50,60,61] and are close to isostructural, approximating to D_{2d} symmetry. These, together with other structures of Group 6 metals with these ligands, are listed in Table 2. The structure of $[Cr_2(mhp)_4]$ is illustrated in Fig. 4. Although the ligand arrangement with D_{2d} symmetry observed for these complexes is the most common coordination arrangement for $[M_2(xhp)_4]$ complexes, it is not the only isomer found. The $[M_2(fhp)_4(THF)]$ complexes have approximately C_{4v} symmetry allowing coordination of a molecule of THF in one axial position [51] (Fig. 5).

Within the triad there is a general increase in metal–metal bond length as the group is descended. For each element, the M–M distance is longer for the chp complexes than for the mhp complexes. Unfortunately, the different structure and the presence of an axial ligand in the fhp complexes prevents a correlation of the M–M distance with the substituent in the 6-position of the pyridone. Two suggestions have been made for the cause of this change in bond length: electron donation from the Cl atoms of chp into an M–M antibonding orbital or an inductive effect of the electronegative substituent weakening the donating ability of the ring nitrogen [50]. It is clear from the structure of the $[M_2(fhp)_4(THF)]$ complexes that the presence of an axial ligand lengthens the M–M bond. Also worth noting is the much greater variation in the M–M bond length for Cr than for either Mo or W.

The replacement of pyridone ligands by non-bridging substituents leads to a slight increase in M–M distance, although the Mo–Mo distances in $[Mo_2(php)_4]$

TABLE 2
Structurally characterized pyridone complexes of Group 6

Formula	Isomer	Oxidation state	Bond order	M–M bond length (Å)	Reference
$[Cr_2(mhp)_4]$	D_{2d}	+2	4	1.879(1)	60
$[Cr_2(mhp)_4].CH_2Cl_2$	D_{2d}	+2	4	1.889(1)	1
$[Cr_2(chp)_4]$	D_{2d}	+2	4	1.955(2)	50
$[Cr_2(fhp)_4(THF)]$	C_{4v}	+2	4	2.150(2)	51
$[Mo_2(mhp)_4]$	D_{2d}	+2	4	2.067(1)	61
$[Mo_2(mhp)_4].CH_2Cl_2$	D_{2d}	+2	4	2.065(1)	1
$[Mo_2(mhp)_4].MeOH$	D_{2d}	+2	4	2.065(1)	61
$[Mo_2(chp)_4]$	D_{2d}	+2	4	2.085(1)	50
$[Mo_2(fhp)_4(THF)]$	C_{4v}	+2	4	2.092(1)	51
$[Mo_2(php)_4]$	C_{2h}	+2	4	2.103(1)	52
$[Mo_2(mhp)_2Cl_2(PEt_3)_2]$	HT	+2	4	2.103(1)	58
$[Mo_2(mhp)_2(O^iPr)_4]$	HT	+3	3	2.206(1)	57
$[Mo_2(mhp)_2(NMe_2)_4]$	HT	+3	3	2.211(2)	56
$[W_2(mhp)_4].CH_2Cl_2$	D_{2d}	+2	4	2.161(1)	1
$[W_2(chp)_4]$	D_{2d}	+2	4	2.177(1)	50
$[W_2(fhp)_4(THF)]$	C_{4v}	+2	4	2.185(2)	51
$[MoW(mhp)_4].CH_2Cl_2$	D_{2d}	+2	4	2.091(1)	71

HT, head-to-tail.

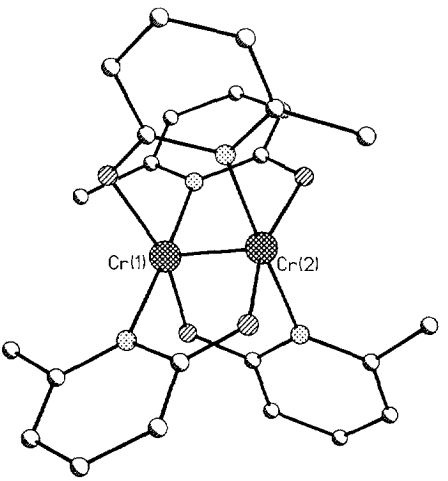

Fig. 4. The structure of $[Cr_2(mhp)_4]$ in the crystal (based on data from ref. 1).

and $[Mo_2(mhp)_2Cl_2(PEt_3)_2]$ are the same. Increasing the oxidation state of the metal to +3 leads to a further increase in the bond length, consistent with removing two electrons from the δ-bonding orbital, thus giving a triple rather than a quadruple bond. To date, such compounds are restricted to Mo; in both $[Mo_2(NMe_2)_4(mhp)_2]$

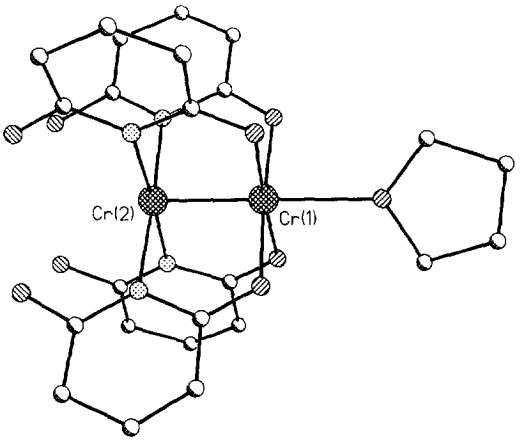

Fig. 5. The structure of $[Cr_2(fhp)_4(THF)]$ in the crystal (based on data from ref. 51).

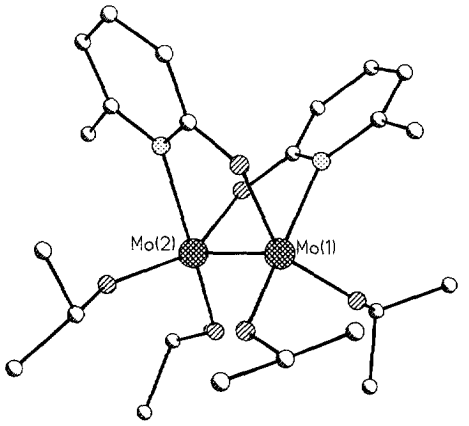

Fig. 6. The structure of $[Mo_2(mhp)_2(O^iPr)_4]$ in the crystal (based on data from ref. 57).

[56] and $[Mo_2(O^iPr)_4(mhp)_2]$ [57], the mhp ligands take up a head-to-tail arrangement about the triple bond (Fig. 6).

The monometallic complex $[Cp_2Mo(hp)][PF_6]$ [59] possesses a chelating pyridone with Mo–O and Mo–N bond lengths of 2.142(10) and 2.138(11) Å respectively. It is structurally similar to two ruthenium complexes discussed in Section 7.3.

5.3. *Physical studies*

The physical properties of these materials have been examined with particular reference to the nature of the metal–metal multiple bonds (triple in the case of M^{3+} and quadruple in the case of M^{2+}).

The mass spectra of the complexes $[M_2(xhp)_4]$ have been examined extensively by Cotton et al. [1,51] and illustrate the high thermal stability (probe temperature, 300°C) of these complexes. The mass spectra typically show a strong parent ion $[M_2(xhp)_4]^+$, with characteristic isotopic distribution patterns. Weaker fragments are also observed for $[M_2(xhp)_4]^{2+}$ and ligand radicals. The stability of these dimers is carried through to the M^{3+} state where, for example, parent ion peaks are observed for $[Mo_2(mhp)_2(NMe_2)_4]^+$ and $[Mo_2(mhp)_4(NMe_2)_2]^+$ [56].

The Raman spectra of $M_2(xhp)_4$ show low-frequency absorptions which were initially attributed to the M–M stretching frequency of the D_{2d} molecule [1]. From these vibrations at 556, 425 and 295 cm^{-1}, the M–M force constants were estimated to be 4.73, 5.70 and 4.71 mdyn $Å^{-1}$ for Cr, Mo and W respectively [1]. However, subsequent work [62] has shown that another absorption at 340 cm^{-1} is better assigned to the Cr–Cr vibration. The set of amended M–M stretching frequencies are in general agreement with the vibrational fine structure observed for bands in the electronic absorption and emission spectra [62]. The presence of donor solvents such as THF leads to a lowering of the anticipated ν_{M-M} presumably via weakening of the M–M bond caused by donation into the M–M δ^* orbitals [1,62]. Replacement of mhp by chp in $[Mo_2(xhp)_4]$ leads to an increase in the M–M bond length and also to a lowering of ν_{M-M} by some 20 cm^{-1} [62]. This has also been attributed to donation from lone pairs on the Cl of chp into M–M δ^* orbitals [62].

UV–visible spectra of the M^{2+} complexes $M_2(xhp)_4$ show three distinct regions [53,54,62]: an α region (22 500, 20 400 and 18 700 cm^{-1} for M≡Cr, Mo and W respectively), which has been attributed to a δ–δ^* transition and often exhibits a vibrational fine structure due to the M–M stretch, a β region attributed to a δ–π^* transition and a γ region above 34 000 cm^{-1} which is ligand based and has a high extinction coefficient (above 23 000 M^{-1} cm^{-1}). The intensity of the α absorption appears to be dependent on the metal, and this has been attributed to an increased configuration interaction for Mo and W. For heavier metals, with greater orbital overlap, this should lead to both a lower energy for the transition and to greater molar absorption coefficient [62]. Other M^{2+} complexes, such as $[Mo_2(mhp)_2Cl_2(PEt_3)_2]$, also show low-energy δ–δ^* transitions, although higher energy transitions are more difficult to assign as they are composed of ligand-localized π–π^* and metal-to-ligand charge transfer (MLCT) transitions [57].

Photoelectron spectra of $M_2(mhp)_4$ complexes have also been reported [63–66] and compared with the spectra of the free ligand Hmhp. The three bands observed are listed in Table 3 and have been assigned on the basis of calculations. The first band is due to ionization from the metal–metal δ-bonding orbital. The second band is associated with ionizations from the metal–metal σ- and π-bonding orbitals, plus some ligand ionizations. The third band is due to predominantly ligand-based ionizations. The ionization potentials of the M–M δ electrons correlate with the $E_{1/2}$ oxidation potentials [65]. Calorimetric studies [67] have determined the enthalpies

TABLE 3
Physical properties of $M_2(mhp)_4$ complexes

Proprety	Cr_2	Mo_2	W_2	CrMo	MoW
Raman					
ν_{M-M} (cm^{-1})	340	425	295	504	384
Force constant (mdyn $Å^{-1}$)		5.70	4.71	5.04	5.47
UV–visible					
λ_{max} (cm^{-1})					
(ε (M^{-1} cm^{-1}))					
δ–δ^*	22500	20400	18700	nr	nr
	(480)	(2100)	(17000)		
δ–π^*	29600	24700	19800		
	(3400)	(12000)	(18500)		
PES (eV)					
δ (M–M)	6.8	5.89	5.3	6.0	5.60
π (M–M)	7.75	7.69	7.70	7.73	7.70
L_π	8.1	8.20	8.0	8.15	8.15
L_π	9.8	9.6	9.6	9.7	9.6
σ	10.2	10.5	10.6	10.5	10.4
L	11.1	11.2	11.3	11.2	11.2
$E_{1/2}$ vs. SCE (V)	+1.01	+0.20	−0.35	+0.35	−0.16

PES, photoelectron spectra; SCE, saturated calomel electrode; nr, not recorded.

of formation in the condensed phase of a series of mhp complexes, and the sublimation enthalpies.

5.4. *Reactivity*

The most common reaction of $[M_2(xhp)_4]$ complexes is ligand substitution in which one or more of the pyridone ligands is replaced by other coordinating groups. For example, reaction of $[Mo_2(mhp)_4]$ with Me_3SiCl in the presence of PEt_3 leads to three products with $[Mo_2(mhp)_2Cl_2(PEt_3)_2]$ being the major product (yield, 60%) [58]. Two other minor products, $[Mo_2(mhp)Cl_3(PEt_3)_3]$ and $[Mo_2(mhp)_3Cl(PEt_3)]$, were identified but not structurally characterized. Attempts to purify $[Mo_2(mhp)_2Cl_2(PEt_3)_2]$ by high vacuum sublimation led only to loss of PEt_3 and the formation of a compound formulated as the tetrameric complex $[Mo_4(mhp)_4Cl_4]$, although there was again no structural determination.

Similar substitution can occur with HX (≡Cl, Br) in the presence of CsX [68] or Li(map) (Hmap = 6-methyl-2-amino-pyridine) [69]

$$Mo_2(mhp)_4 + 4HX + 4CsX \rightarrow Cs_4Mo_2X_8 + 4Hmhp$$

$W_2(mhp)_4 + 4Li(map) \rightarrow W_2(map)_4 + 4Li(mhp)$

It should be noted that reaction of $[W_2(mhp)_4]$ with HX/CsX in methanol leads to oxidative substitution [68]

$W_2(mhp)_4 + 6HX + 3CsX \rightarrow Cs_3W_2X_9 + 4Hmhp + H_2$

or in the presence of phosphine [68]

$W_2(mhp)_4 + 4HX + 6MeOH \rightarrow W_2X_4(OMe)_2(MeOH)_4 + 4Hmhp + H_2$

Chromium(II) complexes also show a tendency to undergo oxidation. For example, $[Cr_2(mhp)_4]$ undergoes oxidative hydrolysis to form the tetrameric complex $[Cr_4(OH)_4(mhp)_8]$ [70]. The reaction requires small, adventitious quantities of water. Excess water leads to the formation of Cr_2O_3. The green discolouration of old samples of $[Cr_2(mhp)_4]$ is likely to be due to the formation of this tetramer. The structure is shown in Fig. 7. It consists of a central Cr_4O_4, cube, with four mhp ligands bridging between two Cr atoms on four faces of the cube, while the remaining four mhp ligands bridge Cr–O edges on two opposing faces. The resultant Cr–Cr distances (2.829(1) and 2.974(1) Å) are around 1 Å longer than those found in $[Cr_2(mhp)_4]$. The d^3 chromium centres are antiferromagnetically coupled, as shown by a study of the magnetic properties of the complex [70].

5.5. *Heterometallic complexes of the chromium triad*

Heterometallic complexes with the formula $[MM'(mhp)_4]$ were originally prepared using techniques analogous to the preparation of the homometallic complexes [71]. For example, a mixture of $Mo(CO)_6$ and $W(CO)_6$ was refluxed in diglyme in the presence of Hmhp, giving the heterometallic complex in greater than 50%

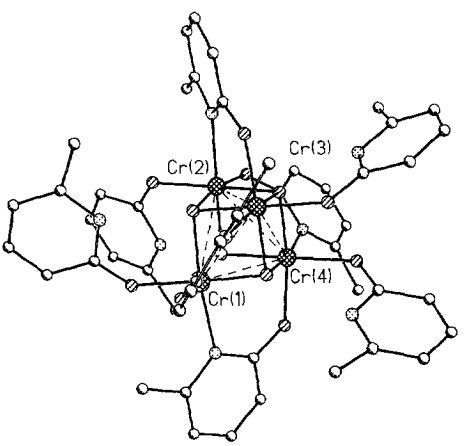

Fig. 7. The structure of $[Cr_4(OH)_4(mhp)_8]$ in the crystal (based on data from ref. 70).

recovered yield [71]. Under suitable conditions, formation of $[W_2(mhp)_4]$ can be excluded and $[Mo_2(mhp)_4]$ can be separated by the selective oxidation of the MoW complex with iodine, followed by purification and subsequent reduction. $[MoW(mhp)_4]$ is isomorphous with the homometallic complexes and possesses a short Mo–W bond of 2.091(1) Å, which is intermediate between the M–M bond lengths in $[Mo_2(mhp)_4]$ and $[W_2(mhp)_4]$. The physical properties of $[MoW(mhp)_4]$ are also intermediate between those of the two homometallic complexes. The Cr–Mo analogue was prepared by reaction of $[CrMo(OAc)_4]$ with Na(mhp) in EtOH, but it has not been isolated free of $[Mo_2(mhp)_4]$ or structurally characterized [65]. To date, there have been no reports of the final heterometallic complex of this triad $[CrW(mhp)_4]$.

Very recently, the synthesis of $[Mo_2(php)_4]$ has allowed access to a highly unusual heterometallic linear tetramer with the formula $[Mo_2(php)_4Pd_2Cl_4]$ (Fig. 8) [52,72].

6. THE MANGANESE TRIAD

As with many of the first-row transition metals, the coordination chemistry of pyridones with manganese has been little studied and no pyridone complexes of manganese have been reported to date. A recent report [73] of the reaction of a mixed-valent trinuclear manganese complex with 2-pyridone has appeared; however, hp is not found in the final product and its role appears to be restricted to promoting isomerization of the initial compound into a new mixed-valent manganese complex.

6.1. *Technetium complexes*

A mixed-valent technetium complex of hp has been reported [74]. It is a highly unusual polymeric compound in which the repeat unit is $[Tc_2(hp)_4Cl]$ (Fig. 9). The

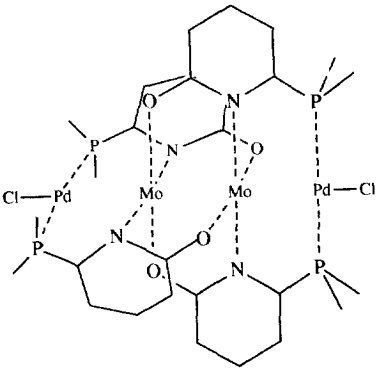

Fig. 8. A schematic diagram showing the structure of the tetranuclear complex $[Mo_2Pd_2(php)_4Cl_2]$ (based on data from ref. 72).

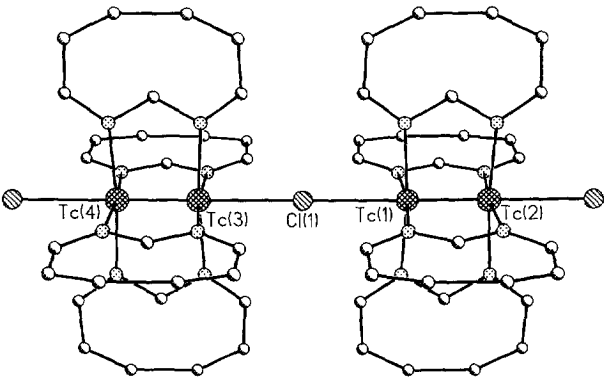

Fig. 9. The structure of the disordered polymer $[Tc_2(hp)_4Cl]$ in the crystal (based on data from ref. 74).

bridging between dimers is via the Cl^- ligand, which occupies the axial position of neighbouring dimers. The dimer has crystallographic D_{4h} symmetry which requires the hp ligands to be completely disordered. The Tc–Tc bond length of 2.095(2) Å is shorter than the metal–metal bond in Re_2^{6+} dimers (see following section). This is perhaps surprising as the formal bond order is higher for the rhemium complexes.

6.2. *Rhemium complexes*

A series of Re_2^{6+} complexes of pyridones have been prepared, in addition to a number of monomeric Re(IV) and Re(V) complexes.

The Re_2^{6+} complexes are readily prepared [75–77] by partial substitution of other ligands (particularly Cl^- and $RCOO^-$) from dimeric complexes such as $[Re_2(OAc)_4Cl_2]$ and $[^tBu_4N]_2[Re_2Cl_8]$ by xhp^-. As with complexes of other triads, the extent of substitution appears to be highly dependent on the reaction conditions employed. Thus $[Re_2(OAc)_4X_2]$ ($X \equiv Cl$, Br) reacts with Hhp or Hmhp in refluxing THF to give $[Re_2(xhp)_2X_4(Hxhp)]$ [75]. The Hxhp ligand is in an axial site and can be displaced by 4-methylpyridine (4-Mepy) to give $[Re_2(xhp)_2X_4(4\text{-Mepy})]$ complexes [75]. In acetonitrile, propionitrile or acetone, $[Re_2(hp)_4X_2]$ species are formed for the unsubstituted ligand, but mixed-bridged species $[Re_2(mhp)_2(O_2CR')X_3]$ are formed ($R' \equiv$ Me or Et) for mhp [75]. The bridging carboxylate is thought to be derived from hydrolysis of the solvent. Both of these latter complexes are thought to develop via $[Re_2(xhp)_2X_4]$ species which are formed as intermediates. $[Re_2(hp)_4Cl_2]$ was originally synthesized from $[Re_2Cl_8]^{2-}$ in molten Hhp [76], and has also been made from reaction of $[Re_2Cl_8]^{2-}$ with Hhp in refluxing 1-pentanol [77]. The reaction of $[Re_2Cl_8]^{2-}$ in molten Hchp gives $[Re_2(\mu\text{-chp})_2(\eta^2\text{-chp})Cl_3]$ in which two of the chp ligands are bridging and one chelating (see below) [78].

Four of these complexes have been structurally characterized and are listed in

Table 4 together with data for $[Tc_2(hp)_4Cl]_n$. Each of the Re complexes contains a formal metal–metal quadruple bond, as for the $[M_2(xhp)_4]$ complexes of Group 6 metals. Within this limited number of compounds, there does not appear to be any systematic variation in bond length. It is expected, based on the results with other triads, that the M–M bond distance should be shortest when the number of bridging ligands is maximized and the number of axial ligands is minimized. Here the shortest bond occurs for the doubly-bridged complex $[Re_2(\mu\text{-chp})_2(\eta^2\text{-chp})Cl_3]$ with one axial ligand (Fig. 10). This complex is unusual in that it possesses both bridging and chelating chp ligands.

The only complex with four bridging ligands is $[Re_2(hp)_4Cl_2]$ [76]. Although both metals are bound to two nitrogens and two oxygens, the ligands are arranged cis about each metal, rather than trans. The C_{2h} isomer is therefore present, rather than the D_{2d} isomer found for $[M_2(mhp)_4]$, where M ≡ Cr, Mo, W. For the three complexes structurally characterized with two bridging ligands, in each case the xhp

TABLE 4

Structurally characterized pyridone complexes of Group 7

Formula	Isomer	No. of axial L	M–M bond length (Å)	Reference
$[Tc_2(hp)_2Cl]_n$	[a]	2	2.095(2)	74
$[Re_2(hp)_4Cl_2]$	C_{2h}	2	2.206(2)	76
$[Re_2(mhp)_2Cl_4(Hmhp)].CH_3COCH_3$	HH	1	2.2096(9)	75
$[Re_2(mhp)_2(O_2CEt)Cl_3]$	HH	1	2.2041(6)	75
$[Re_2(\mu\text{-chp})_2(\eta^2\text{-chp})Cl_3].CH_2Cl_2$	HH	1	2.2015(7)	78

[a] The core is Tc_2^{5+} and the ligands are completely disordered (see text).
HH, head-to-head.

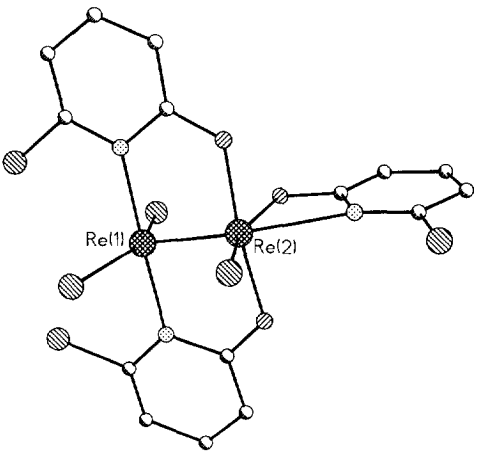

Fig. 10. The structure of the asymmetric dimer $[Re_2(chp)_3Cl_3]$ in the crystal (based on data from ref. 78).

ligands are arranged head-to-head (HH). This allows formation of a further bond in the axial site of the complex (see Fig. 10).

Physical studies of these complexes are restricted to electronic absorption spectroscopy [75,77] and electrochemical studies [75]. Highest occupied molecular orbital–lowest unoccupied molecular orbital (HOMO–LUMO) (δ–δ^*) transitions typically occur in the region 14045–16835 cm^{-1}, with other transitions (ligand-to-metal charge transfer (LMCT) and intraligand π–π^*) also observed at higher energy. The electrochemistry for a series of complexes with the formulae $[Re_2(xhp)_2X_4(L)]$ (xhp ≡ hp, mhp; X ≡ Cl, Br; L ≡ Hhp, Hmhp, 4-Mepy) and $[Re_2(O_2CR')(mhp)_2X_3]$ (R′ ≡ Me, Et; X ≡ Cl, Br) has been reported [75]. For the former series, oxidation is observed at about +1.5 V (near the solvent limit) and reduction at about −0.42 V. For the latter complexes, only reduction is observed at about −0.59 V (all potentials vs. Ag/AgCl). The ^1H NMR spectra of these complexes have also been reported [75].

In addition to this chemistry, some work on the reactions of $[ReH_7(PPh_3)_2]$ with Hhp and Hmhp has recently been reported [79,80]. This was part of a study of the reactivity of rhenium polyhydrides with organic acids, the intention being to produce H_2 and an unsaturated Re coordination sphere. The initial product of these reactions is $[ReH(xhp)_2(PPh_3)_2]$ [79]. These complexes were characterized by NMR spectroscopy and their redox chemistry was examined. They undergo a reversible oxidation at about −0.04 V (vs. Ag/AgCl), and can be chemically oxidized to a purple monocation, $[ReH(xhp)_2(PPh_3)_2]^+$ with $[(C_5H_5)_2Fe]^+$ as oxidant [79]. The cation can be reduced using $[(C_5H_5)_2Co]$.

Additional reactions of $[ReH(xhp)_2(PPh_3)_2]$ include protonation with HPF_6 to give $[ReH_2(xhp)_2(PPh_3)_2](PF_6)$. For xhp ≡ mhp, structural determination found the trans isomer of this complex; for xhp ≡ hp, the cis isomer was structurally characterized [80]. These complexes can be deprotonated using standard reagents, e.g. NEt_3. On attempting to crystallize $[ReH(mhp)_2(PPh_3)_2](PF_6)$, green crystals of $[ReO(mhp)_2(PPh_3)_2](PF_6)$ are formed. X-Ray analysis revealed the trans isomer of this complex. In all the crystallographically characterized compounds, the xhp ligands are found to be chelating [80]

7. THE IRON TRIAD

As with the previous triads, the chemistry of Group 8 metals with 2-pyridone ligands is dominated by the formation of dimeric complexes. No work has been reported for iron, other than the crystal structures of $[Fe(xhp)_6][NO_3]_3$ (xhp ≡ hp, mhp) [36,37] and the formation of $[Fe(3\text{-}OHhp)_3]$ [23]. The work on dimeric osmium and ruthenium compounds is, however, quite extensive. There is also a small body of work on mononuclear ruthenium complexes.

7.1. Synthesis and structures of dimeric Os and Ru complexes

The crystallographically characterized compounds of this class are listed in Table 5. The range of oxidation states is wider than for any other triad, varying from

TABLE 5
Structurally characterized pyridone complexes of ruthenium and osmium

Formula	Isomer	Oxidation state	Bond order	M–M bond length (Å)	Reference
$[Ru_2(hp)_2(CO)_4(Hhp)_2]$	HT	+1	1	2.670(1)	83
$[Ru_2(hp)_2(CO)_4(PPh_3)_2]$	HT	+1	1	2.7108(6)	84
$[Ru_2(mhp)_4].CH_2Cl_2$	D_{2d}	+2	2	2.238(1)	85,86
$[Ru_2(mhp)_4]$	D_{2d}	+2	2	2.235(1)	87
$[Ru_2(bhp)_4].1.5C_6H_6$	D_{2d}	+2	2	2.259(1)	87
$[Ru_2(chp)_4]_2$	3:1	+2	2	2.247(1)	87
$[Ru_2(fhp)_4(THF)]$	C_{4v}	+2	2	2.274(1)	88
$[Ru_2(hp)_4Cl(Hhp)]$	C_{4v}	+2.5	2.5	2.286(1)	89
$[Ru_2(chp)_4Cl]$	C_{4v}	+2.5	2.5	2.281(1)	90
$[Ru_2(fhp)_4Cl]$	C_{4v}	+2.5	2.5	2.284(1)	91
$[Ru_2(mhp)_2(OAc)_2Cl].0.5CH_2Cl_2$	HH	+2.5	2.5	2.278(2)	92
$[Ru_2(chp)_3(OAc)Cl]CH_2Cl_2$	HH	+2.5	2.5	2.282(4)	93
$[Os_2(chp)_4Cl]$	C_{4v}	+2.5	2.5	2.348(1)	82
$[Os_2(fhp)_4Cl]$	C_{4v}	+2.5	2.5	2.341(1)	94
$[Os_2(hp)_4Cl_2].Et_2O$	D_{2d}	+3	3	2.344(2)	2
$[Os_2(hp)_4Cl_2].CH_3CN$	D_{2d}	+3	3	2.357(1)	2
$[Os_2(hp)_2Cl_4(py)]$	HH	+3	3	2.322(1)	95
$[Os_2(hp)_2Cl_4(H_2O)].(CH_3)_2CO$	HH	+3	3	2.293(1)	95

py, pyridine.

complexes which have Ru_2^{2+} cores to those with Os_2^{6+} cores. For this triad, and for the complexes discussed here, the metal–metal bond order coincides with the metal oxidation state.

The first such compound reported was the osmium dimer, $[Os_2(hp)_4Cl_2]$ [2,81], synthesized by reaction of Hhp with osmium trichloride in ethanol. Two different solvates of this compound have been crystallographically characterized and, in both cases, the isomer found has approximate D_{2d} symmetry (Fig. 11). The two chloride ligands occupy axial positions. No osmium complex of 2-pyridone ligands has been reported which does not feature at least one axial ligand. Even the use of chp as a ligand leads to a "polar" arrangement of ligands, e.g. in $[Os_2(chp)_4Cl]$ (Fig. 12), with the four chp nitrogens attached to one metal and the four chp oxygens attached to the second. This geometry allows one axial Cl to be present [82]. No complex with osmium in an oxidation state lower than +2.5 has been characterized.

In some ways the opposite is true of the ruthenium complexes. The first reported was $[Ru_2(mhp)_4]$, which has ruthenium in the +2 oxidation state, and contains no axial ligands [85]. The work on Ru dimers since this report has led to a series of complexes with the metal core varying from Ru_2^{2+} to Ru_2^{5+}, but with no examples of the M_2^{6+} core found for osmium.

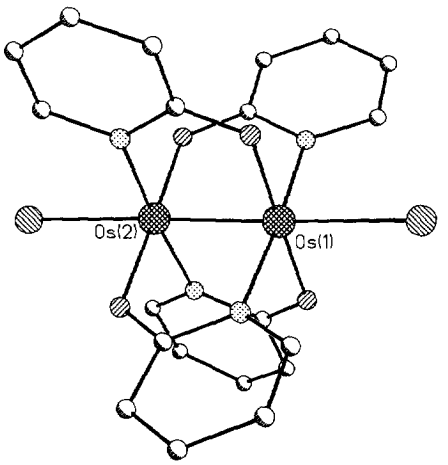

Fig. 11. The structure of $[Os_2(hp)_4Cl_2]$ in the crystal (based on data from ref. 2).

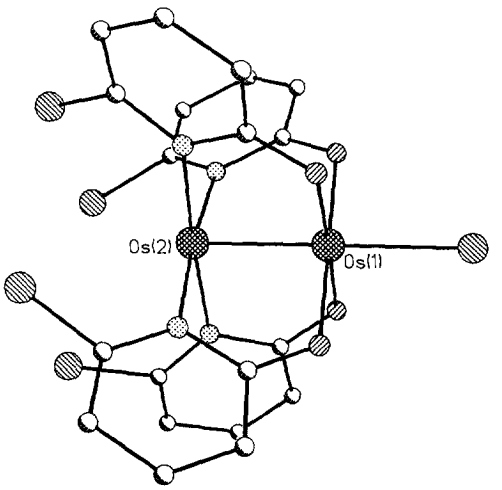

Fig. 12. The structure of $[Os_2(chp)_4Cl]$ in the crystal (based on data from ref. 82).

The majority of these complexes have been made by the replacement of acetate ligands in dimeric precursors. Only one example of the synthesis of a dimeric ruthenium or osmium pyridone complex from a mononuclear precursor exists [2], and that is the formation of $[Os_2(hp)_4Cl_2]$ from osmium trichloride. For ruthenium, the most common precursor has been $[RuCl(OAc)_4]$ [85,89–93] which is, in general, reacted with the neutral Hxhp ligand, either in the molten ligand as solvent [89–91] or in refluxing alcohols [93]. In these reactions incorporation of Cl^- in the final

product is almost always observed. Reaction of $[Ru_2Cl(OAc)_4]$ with Na(mhp) in methanol gives $[Ru_2(mhp)_4]$, but only in 8% yield [85].

Synthesis of osmium dimers has largely been based on the reaction of $[Os_2Cl_2(OAc)_4]$ in molten Hxhp [82,95], and again incorporation of chloride in the isolated product is always observed. More recently, the availability of the homoleptic $[M_2(OAc)_4]$ complexes [96] has allowed access to dimeric pyridone complexes which do not contain coordinated chloride [87,88]. This has led to an improved synthesis of $[Ru_2(mhp)_4]$ [87], and to new species such as $[Ru_2(bhp)_4]$, $[Ru_2(chp)_4]_2$ [87] and $[Ru_2(fhp)_4(THF)]$ [88]. The Ru_2^{2+} complexes were also prepared by replacement of acetate from dimeric precursors [83,84].

An interesting feature of the pyridone coordination chemistry of Os and Ru is the contrast between the two metals. The only common species are $[M_2(fhp)_4Cl]$ [91,94] and $[M_2(chp)_4Cl]$ [82,90] (cf. Mo and W). In both cases, the Ru–Ru bond is around 0.06 Å shorter than the Os–Os bond (see Table 5). All other osmium complexes contain an M_2^{6+} core which has yet to be observed for ruthenium pyridone complexes. No osmium complexes of the mhp ligand have been reported, which is surprising giving its importance in dimeric complexes of other metals.

For ruthenium, there is a considerable bond length range from 2.235(1) Å for $[Ru_2(mhp)_4]$ [87] to 2.7108(4) Å for $[Ru_2(hp)_2(CO)_4(PPh_3)_2]$ [84]. The longest bonds occur for the complexes with an Ru_2^{2+} core in which the bond order is unity and the electronic configuration is $\sigma^2\pi^4\delta^2\delta^{*2}\pi^{*4}$. (The energies of δ^* and π^* orbitals are very close and the exact order of the energy levels is unclear.) However, the shortest bonds occur for complexes where the bond order is two, e.g. $[Ru_2(mhp)_4]$, and not for complexes where the bond order is 2.5, e.g. $[Ru_2(chp)_4Cl]$ [90]. Unfortunately, few direct comparisons can be made; however, comparing $[Ru_2(fhp)_4(THF)]$ with $[Ru_2(fhp)_4Cl]$ or $[Ru_2(chp)_4]_2$ with $[Ru_2(chp)_4Cl]$ supports this observation. In both cases, the double bond is shorter (by 0.010(1) and 0.034(1) Å respectively) than the bond of order 2.5. This observation becomes important in deciding on the precise electronic configuration for the Ru_2^{4+} complexes (see below).

Three isomers have been observed for the quadruple-bridged dimers. The D_{2d} isomer is found for $[Ru_2(mhp)_4]$ and $[Ru_2(bhp)_4]$ [85,87], and also for $[Os_2(hp)_4Cl_2]$ [2]. The fhp complexes are all found as the C_{4v} isomer, as for metals of other triads; however, surprisingly, this isomer is also found for both $[Os_2(chp)_4Cl]$ [82] and $[Ru_2(chp)_4Cl]$ [90]. There would appear to be considerable steric crowding between the chloro substituents, although they do not come with the van der Waals' radii of each other (Fig. 12), and this in turn suggests a considerable driving force for coordination of an axial ligand to these metal dimers. In $[Ru_2(chp)_3(OAc)Cl]$, the three bridging chp ligands are again arranged head-to-head to allow coordination of Cl. The third isomer observed is the 3:1 arrangement of ligands found for $[Ru_2(chp)_4]_2$ [87], which again allows axial coordination, this time from a μ_2-pyridone oxygen (Fig. 13). This leads to a dimer of dimers being formed.

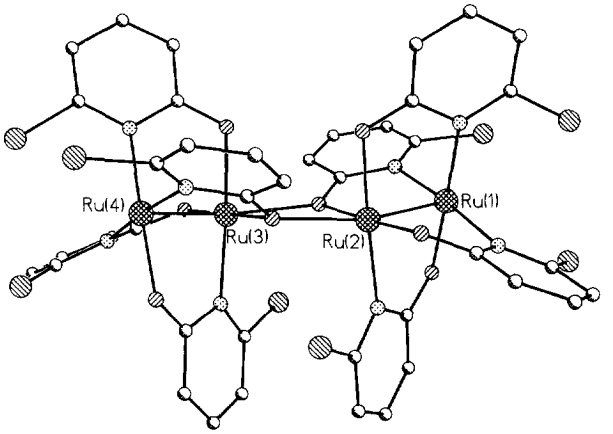

Fig. 13. The structure of the dimer of dimers $[Ru_2(chp)_4]_2$ in the crystal (based on data from ref. 87).

A further feature of this triad is the occurrence of mixed-bridged complexes [92,93] and complexes which contain only two bridging pyridones [83,84,95]. In every case, this is caused by incomplete substitution of acetate, chloride or carbonyl ligands in the dimeric precursor. In the Ru_2^{2+} complexes, which both contain hp, the head-to-tail isomer is found, while for the complexes of higher oxidation states, which contain either mhp or chp ligands, the head-to-head isomer is found which allows coordination of an axial ligand.

7.2. *Physical studies*

Many of the physical studies of this class of compounds have been dedicated to establishing the exact electronic configuration within the metal–metal bonding and antibonding orbitals. While all are agreed that the first eight electrons involved must occupy σ-, π- and δ-bonding orbitals, the energies of the δ^*- and π^*-antibonding orbitals are sufficiently close that it is not immediately obvious which should be occupied first. For example, the first of these complexes reported, $[Os_2(hp)_4Cl_2]$, has a magnetic moment of 1.44 Bohr magneton (μ_B) per formula unit, which is clearly inconsistent with an isolated $\sigma^2\pi^4\delta^2\delta^{*2}$ ground state; presumably the $\sigma^2\pi^4\delta^2\delta^{*1}\pi^{*1}$ state is also occupied at room temperature.

The only photoelectron spectrum reported for these complexes is that of $[Ru_2(mhp)_4]$ [85]. Five bands are observed which, in order of decreasing energy, are assigned as ionizations from (i) the Ru–Ru π-bonding orbital, (ii) a ligand-based π orbital, (iii) the Ru–Ru δ orbital, (iv) the Ru–Ru δ^* orbital and (v) the Ru–Ru π^* orbital. This indicates that both the π^* and δ^* orbitals are occupied. The magnetic moment of this complex is $2.9\mu_B$ per formula unit at room temperature, which is very close to the spin-only value for two unpaired electrons. The relevance of the spin-only value must be limited in a system of this complexity. The two possible

configurations for the Ru_2^{4+} core which are consistent with these observations are $\sigma^2\pi^4\delta^2\delta^{*1}\pi^{*3}$ and $\sigma^2\pi^4\delta^2\delta^{*2}\pi^{*2}$. SCF-$X_\alpha$ calculations on $[Ru_2(O_2CH)_4]$ suggested the former configuration as the ground state [97]; however, this conclusion seems questionable based on two more recent pieces of evidence.

The first is the observation, mentioned above, that the Ru–Ru bond length is longer in Ru_2^{5+} complexes than in Ru_2^{4+} complexes, despite the fact that the latter complexes contain an additional electron in an antibonding orbital. This is best explained by assuming that this additional electron eners a δ^* orbital rather than a π^* orbital, which would be expected to have a greater effect on the M–M distance. This would lead to the electronic configurations of $\sigma^2\pi^4\delta^2\delta^{*1}\pi^{*2}$ and $\sigma^2\pi^4\delta^2\delta^{*2}\pi^{*2}$ for Ru_2^{5+} and Ru_2^{4+} respectively. The second piece of evidence comes from variable-temperature magnetic measurements on $[Ru_2(mhp)_4]$, $[Ru_2(bhp)_4]$, $[Ru_2(chp)_4]_2$ [87] and $[Ru_2(fhp)_4(THF)]$ [88]. At very low temperature, the magnetic moment for these complexes tends to zero, which is only consistent with a diamagnetic ground state. For the $\sigma^2\pi^4\delta^2\delta^{*2}\pi^{*2}$ ground state, the spin triplet ($M_s=0,\pm1$) ground state would be expected to undergo zero-field splitting to give a spin singlet ($M_s=0$) state and a spin doublet ($M_s=\pm1$) state. If the spin singlet state is the ultimate ground state, the complexes would become diamagnetic at low temperature while at higher temperatures the magnetism would be that due to two unpaired electrons. This matches the observed behaviour very well [87,88]. If the ground state were $\sigma^2\pi^4\delta^2\delta^{*1}\pi^{*3}$, the magnetic behaviour would be quite different and the magnetic moment should not be so sensitive to a variation in temperature [88]. Assuming that the former explanation is correct, the size of this splitting can be calculated. The zero-field splitting parameter varies from 208 cm^{-1} for $[Ru_2(mhp)_4]$ [87] to 262 cm^{-1} for $[Ru_2(fhp)_4(THF)]$ [88].

The electronic spectra of these complexes are dominated by an allowed transition from a ligand-based π orbital to an M–M π^* orbital. The electrochemistry of these complexes has also been examined. For ruthenium, studies of two Ru_2^{5+} complexes have been reported [91,92], which both reveal a quasi-reversible one-electron oxidation at about +1.66 V and a reversible one-electron reduction at about −0.05 V. Additionally, $[Ru_2(CO)_4(hp)_2L_2]$ complexes (L ≡ PPh_3, P^iPr_3, Hhp) [83], which contain the Ru_2^{2+} core, show a one-electron oxidation to Ru_2^{3+} at about +0.40 V for L ≡ phosphine and +1.11 V for L ≡ Hhp. These electrochemical experiments therefore complete the series of Ru_2^{n+} complexes, with reports existing of ruthenium dimer cores for $n=2$–6. Neither Ru_2^{3+} nor Ru_2^{6+} complexes have been isolated and fully characterized, although an EPR spectrum of an Ru_2^{3+} complex has been reported [83].

For osmium, the electrochemical experiments have been restricted to two types of complex. For $[Os_2(hp)_4X_2]$ (X ≡ Cl, Br) [98,99], a one-electron oxidation at about +1.31 V and a one-electron reduction at about +0.18 V are observed. This oxidation generates an Os_2^{7+} core, which is again a core which has not been isolated. For $[Os_2(xhp)_4Cl]$ (xhp ≡ chp, fhp) [82,94] a one-electron oxidation at about +0.92 V

and a one-electron reduction at about −0.61 V are observed. The reduction generates an Os_2^{4+} core, the complexes of which have not been fully characterized for these ligands. Thus, including the electrochemically generated species, evidence exists for Os_2^{n+} complexes for $n=4$–7. The EPR spectra for two Os_2^{5+} complexes at 100 K have been reported [82,100]. In both cases, a well-defined spectrum is observed close to $g=2.2$.

7.3. Other ruthenium complexes

Three mononuclear Ru^{2+} complexes of xhp ligands have been structurally characterized: $Ru(hp)_2(PPh_3)_2$ [101], $Ru(C_6H_6)(hp)Cl$ [102] and Ru(*p*-cymene)(hp)Cl (where *p*-cymene = *p*-$CH_3C_6H_4CH(CH_3)_2$) [103]. In each case, the pyridone ligand chelates with the Ru–N bond (average, 2.09 Å) which is significantly shorter than the Ru–O bond (average, 2.14 Å). This is the opposite order to that observed for dimeric complexes of these ligands. Other related complexes have also been synthesized but not structurally characterized [102,103].

A trinuclear Ru complex featuring hp has also been reported [104]. This is the anion $[Ru_3(\mu_2\text{-}\eta^2\text{-hp})(CO)_{10}]^-$, synthesized from the reaction of either Khp or (PPN)(hp) with $[Ru_3(CO)_{12}]$ or $[Ru_3(\mu\text{-H})(CO)_{11}]^-$. The structure contains a binucleating hp ligand (Fig. 14) with the Ru–Ru edge bridged by hp shorter (at 2.7611(7) Å) than the two unbridged Ru–Ru contacts (average, 2.8585(8) Å). It was hoped that the ability of hp to become trinucleating would labilize one of the carbonyl groups, giving the anion $[Ru_3(\mu_3\text{-}\eta^2\text{-hp})(CO)_9]^-$, which might then undergo substitution. Unfortunately, for hp this reaction is very slow, although for 2-mercaptopyridine the reaction does lead to further substitution of the carbonyl ligands [104].

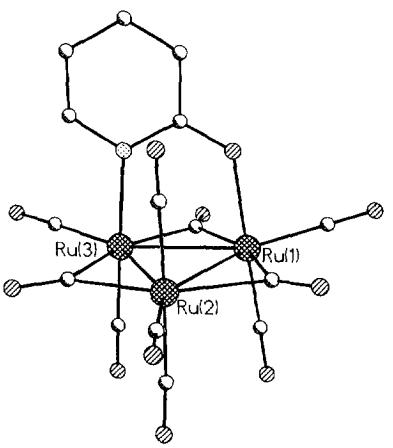

Fig. 14. The structure of the anion $[Ru_3(CO)_{10}(hp)]^-$ in the crystal (based on data from ref. 104).

8. THE COBALT TRIAD

8.1. Cobalt complexes

Similar to the manganese and iron triads, there has been more work carried out on the complexes of the heavier elements with pyridone ligands than on the first-row metal. However, there are three accounts of work involving cobalt in the literature [4,37,43,44]. The earliest is work by Gould [43,44] on the rate of linkage isomerism of Hhp when attached to a cobalt(III) centre. The most interesting is work by Clegg et al. [4] which involves the reaction of anhydrous cobalt acetate with the sodium salt of mhp, and also the reaction of anhydrous cobalt acetate with molten Hmhp. Unfortunately, complete characterization by X-ray crystallography was only possible for the product of the latter reaction. The reaction of Na(mhp) leads to a cobalt complex of stoichiometry $[Co(mhp)_2]$ as shown by elemental analysis. This compound is thought to be monomeric both in solution, as shown by the magnetic moment which is consistent with tetrahedral Co(II), and in the gas phase, as shown by mass spectroscopy. The complex is extremely moisture sensitive, decomposing to give Hmhp and a pale blue precipitate on exposure to air. A bipyridyl (bipy) adduct, $[Co(mhp)_2(bipy)]$, can be prepared which is more stable.

The reaction in molten Hmhp gives an extraordinary $[Co_{12}(OH)_6(OAc)_6(mhp)_{12}]$ complex (Fig. 15). The incomplete replacement of acetate ligands is reminiscent of syntheses involving molybdenum (Section 5.1) where acetate can be found to be an impurity. The presence of bridging hydroxide groups presumably arises through incomplete dehydration of cobalt acetate. This complex

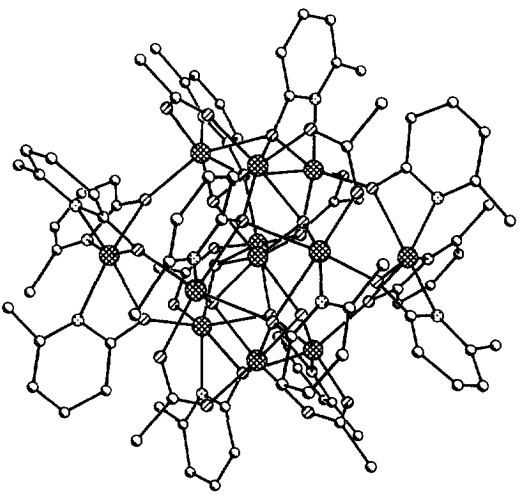

Fig. 15. The structure of the dodecanuclear complex $[Co_{12}(OH)_6(OAc)_6(mhp)_{12}]$ in the crystal (based on data from ref. 4).

has crystallographically imposed C_3 symmetry, and approximate D_3 symmetry. The arrangement of metal atoms involves a distorted trigonal prism of six Co atoms, which contains a seventh Co at its centre, and is capped by further Co atoms on each square and triangular face. As there are three square and two triangular faces this leads to 12 Co atoms.

The compound is held together in a different manner to the dimeric compounds featuring mhp. The hydroxides present all bridge between three Co atoms — the central cobalt and one each of the Co atoms in the prism and those capping the square faces. The mhp ligands each act as a chelating ligand to a cobalt atom, with bridges via the exocyclic oxygen to two further cobalts. The ligands are therefore tetradentate but only trinucleating.

A mononuclear cobalt complex of Hmhp of formula $Co(Hmhp)_4(NO_3)_2$ [37] has also been structurally characterized. The cobalt sits on an inversion centre, and mhp is bound via the oxygen, with the hydrogens attached to the nitrogen involved in intramolecular hydrogen bonding.

8.2. *Dinuclear complexes of rhodium(II)*

The first report of a rhodium complex of pyridone ligands was $[Rh_2(mhp)_4]$ [105,106] (Fig. 16). This was the first of 14 reported crystal structures involving Rh_2^{4+} cores with pyridones which are listed in Table 6. In all of these complexes, the electronic configuration of the Rh_2^{4+} core with respect to metal–metal bonding is $\sigma^2\pi^4\delta^2\delta^{*2}\pi^{*4}$, with a resultant single bond between the rhodium atoms. The metal–metal distance is therefore longer than the metal–metal distance in dimers of earlier transition metals (see Sections 5.1, 6.2 and 7.1). The syntheses of these complexes

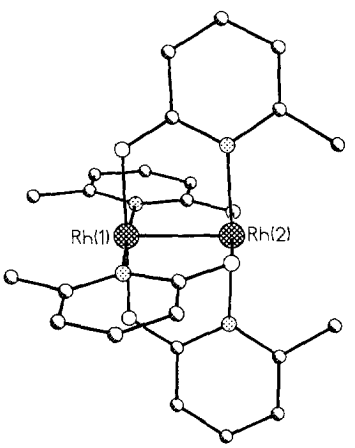

Fig. 16. The structure of $[Rh_2(mhp)_4]$ in the crystal (based on data from ref. 106).

TABLE 6
Structurally characterised Rh complexes with pyridone

Formula	Isomer	No. of axial L	Rh–Rh bond length (Å)	Reference
$[Rh_2(mhp)_4]$	D_{2d}	0	2.359(1)	106
$[Rh_2(mhp)_4].CH_2Cl_2$	D_{2d}	0	2.367(1)	107
$[Rh_2(mhp)_4].H_2O$	D_{2d}	0	2.370(1), 2.365(1)[a]	108
$[Rh_2(chp)_4]$	D_{2d}	0	2.379(1)	108
$[Rh_2(fhp)_4(DMSO)]$	C_{4v}	1	2.410(1)	109
$[Rh_2(mhp)_4(Hmhp)].0.5C_7H_8$	3:1	1	2.383(1)	110
$[Rh_2(mhp)_4(CH_3CN)]$	3:1	1	2.372(1)	108
$[Rh_2(mhp)_4(imid)].0.5CH_3CN$	3:1	1	2.384(1)	108
$[Rh_2(chp)_4(imid)].3H_2O$	3:1	1	2.385(1)	108
$[Rh_2(mhp)_4]_2$	3:1[b]	1	2.369(1)	110
$[Rh_2(mhp)_3(OTs)]_2$	3:1[b]	1	2.377(3), 2.376(3)	111
$[Rh_2(mhp)_2(OAc)_2(imid)]$	HH	1	2.388(2)	108
$[Rh_2(mhp)_2(OAc)_2(imid)].2CH_2Cl_2$	HH	1	2.4439(6)	108
$[Rh_2(chp)_2(OAc)(CH_3CN)_3][BF_4]$	HH	1	2.388(1)	112

[a] Two independent molecules in the asymmetric unit.
[b] The complex is a dimer with an mhp oxygen in the axial position.
DMSO, dimethylsulphoxide; imid, imidazole; OTs, $CH_3C_6H_4SO_3^-$.

have concentrated on the reaction of $RhCl_3.3H_2O$ with sodium salts of the ligands [105,110] or the reaction of $Rh_2(OAc)_4$ in the molten ligand [108,109].

Several trends in the structural chemistry of these dimers can be identified. Firstly, by comparison with other $[M_2(xhp)_4]$ compounds, there is much less dominance of the D_{2d} geometry, with a marked tendency for 3:1 coordination of the pyridones, which allows coordination of one axial ligand. In the absence of a donor solvent, this axial ligation can also be manifested as dimerization of the dimers, where an xhp oxygen becomes μ_2-bridging, binding to one metal in the expected manner and acting as an axial ligand to the second dimer, e.g. in $[Rh_2(mhp)_3(OTs)]_2$ [111] (Fig. 17).

The Rh–Rh bond length range is comparatively narrow. If we exclude $[Rh_2(chp)_2(OAc)(CH_3CN)_3][BF_4]$, which has only three bridging ligands rather than four [112], and $[Rh_2(fhp)_4(DMSO)]$ [109], for less justifiable reasons, the range is only 0.029 Å (from 2.359(1) Å for $[Rh_2(mhp)_4]$ to 2.388(1) Å for $[Rh_2(mhp)_2(OAc)_2(imid)].2CH_2Cl_2$ [108]). The Rh–Rh bond length for the $[Rh_2(mhp)_4]$ unit varies by 0.011 Å depending on the solvate present; therefore the 0.029 Å range seems even narrower and it is dangerous to pick out trends. As the addition of an axial ligand should lead to some occupation of the M–M σ^* orbital, we expect that those complexes with axial ligands should have longer Rh–Rh

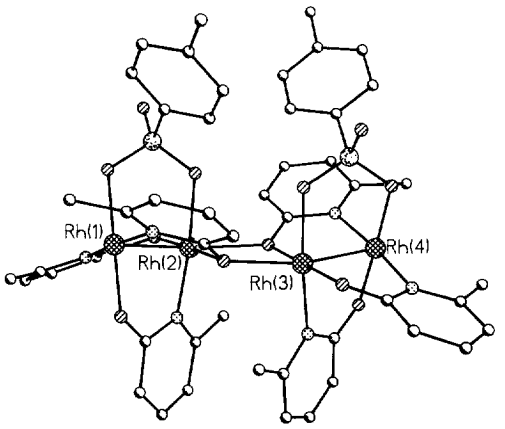

Fig. 17. The structure of the dimer of dimers $[Rh_2(mhp)_3(OTs)]_2$ in the crystal (based on data from ref. 111).

bonds than comparable complexes without. The values can be used to support this argument, but not decisively. It also appears, as for other metals, that the complexes with chp ligands have a longer M–M bond than those with mhp ligands. $[Rh_2(fhp)_4(DMSO)]$ [109] has an unusually long Rh–Rh bond of 2.410(1) Å and the C_{4v} geometry which always occurs for fhp.

In the cases where mixed acetate/pyridone ligands are present, the geometry is such that the pyridone ligands are trans to each other, and also oriented head-to-head, e.g. $[Rh_2(mhp)_2(OAc)_2(imid)]^+$ [108] (Fig. 18). This orientation appears to maximize the interaction between the substituents in the 6-position of the pyridone rings, and it is unclear why this should occur. However, as with Ru and Os complexes where this occurs, it is worth bearing in mind that the substituents are not within

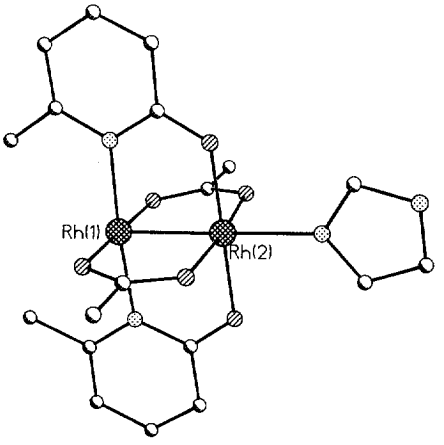

Fig. 18. The structure of $[Rh_2(mhp)_2(OAc)_2(imid)]$ in the crystal (based on data from ref. 108).

van der Waals' contact of each other, and therefore any interaction is likely to be minimal.

Many fewer physical studies have been reported for these Rh_2^{4+} complexes than for the pyridone complexes of Group 6 metals (see Section 5.3), or indeed for Rh_2^{4+} carboxylates [113]. The UV–visible photoelectron spectrum of $Rh_2(mhp)_4$ has been reported [105], which has allowed assignment of the ionization energies of electrons in the metal–metal bonding and antibonding orbitals. The π^* orbitals are lower in energy than the δ^* orbitals, probably because of a strong interaction of the π^* orbitals with the highest filled ligand orbitals.

^{103}Rh NMR spectra have been reported for $[Rh_2(mhp)_4]$ and $[Rh_2(mhp)_4]_2$ [114]. The former compound has two equivalent Rh nuclei and hence only a singlet is observed at $\delta = 5745$ ppm. In the latter compound there are two inequivalent rhodiums, one bound to an N_3ORh donor set and the second to an NO_3Rh donor set. Two doublets are seen in the ^{103}Rh NMR spectrum at about 7644 and 4322 ppm with $J_{Rh-Rh} = 35$ Hz.

An electrochemical study of $[Rh_2(xhp)_4]$ (xhp ≡ hp, chp, mhp) in a variety of solvents has been reported [115]. Each compound undergoes a reversible one-electron oxidation. The potential of this oxidation is dependent on the bridging ligand and on the solvent. For $[Rh_2(chp)_4]$, the oxidation occurs between +1.20 and +1.44 V. For $[Rh_2(mhp)_4]$, the range is between +0.92 and +1.21 V. For $[Rh_2(hp)_4]$, the range is +0.63 to +0.88 V. In each case, the oxidation occurs most readily in pyridine, while it is most difficult in DMSO for $[Rh_2(chp)_4]$, in propylene carbonate for $[Rh_2(mhp)_4]$ and in nitromethane for $[Rh_2(hp)_4]$. An attempt was made to correlate the oxidation potentials with Gutmann's donor number [116] for the various solvents without great success. The oxidation is clearly easiest when "$Rh_2(hp)_4$" is the substrate; however, this compound has not been crystallographically characterized and in a donating solvent is likely to exist as $[Rh_2(hp)_4(sol)_2]$. It has also been shown that the D_{2d} isomer of $[Rh_2(mhp)_4]$ can rearrange in the presence of a donor solvent, e.g. CH_3CN, to give the 3:1 isomer $[Rh_2(mhp)_4(CH_3CN)]$ [108]. Therefore the nature of the species in solution is not entirely clear for any of the three compounds. Drago et al. [117] showed that, for Rh_2^{4+} carboxylates, complexes with two axial ligands are more easily oxidized than complexes with one axial ligand. This may well explain why $[Rh_2(hp)_4]$ is more easily oxidized than the other two complexes.

8.3. Dinuclear complexes of rhodium(I) and iridium(I)

In addition to the body of work described above where d^7 metal centres are bridged by 2-pyridones, there exists a series of complexes in which d^8 rhodium and iridium atoms are linked by such ligands. Whereas in the d^7 complexes pyridones take the place of carboxylate ligands, in the d^8 complexes they are substituted for ligands such as pyrazole (pz).

A preliminary communication of the synthesis, structural characterization and reactivity of $[Ir(COD)(mhp)]_2$ (COD, 1,5-cyclooctadiene) appeared in 1985 [118]. Two full papers expanding on this work have since been published [119,120]. Related publications in this area have appeared from other groups [121–124].

$[Ir(COD)(xhp)]_2$ complexes are prepared via reaction of the Na(xhp) salts with $[Ir(COD)(\mu\text{-}Cl)]_2$ [125] in either THF or dichloromethane [118,119]. The equivalent $[Rh(COD)(xhp)]_2$ complexes are synthesized from the reaction of mononuclear $[Rh(COD)(CH_3CN)_2][BF_4]$ with Na(xhp) [119], or from $[Rh(COD)(\mu\text{-}Cl)]_2$ [122]. Compounds with other bidentate olefin ligands, such as norbornadiene (NBD) [121] and tetrafluorobenzobarrelene [124], can be prepared by similar procedures.

Only three structures of these $[M(diolefin)(xhp)]_2$ complexes have been reported, and all are similar (Fig. 19). Two square planar metal centres are bridged by two pyridones with the coordination sphere of the metal consisting of the chelating η_4-diolefin, the nitrogen from one xhp unit and the oxygen from the second xhp unit. The xhp ligands are cis and oriented head-to-tail. The metal–metal distance varies between 3.367(1) Å for $[Rh(COD)(mhp)]_2$ [119] and 3.040(1) Å for [Rh(NBD)(chp)] [121], and appears to depend on the diolefin present, with the distance lengthening in the former complex because of steric interactions between the COD ligands on the two metals. The M–M distance is 3.242(1) Å in $[Ir(COD)(mhp)]_2$ [119]. This is a larger difference between the homologous iridium and rhodium compounds than in the similar pair of complexes $[M(COD)(pz)]_2$ [126] where the difference is 0.051 Å; this indicates the greater flexibility of three-atom bridging ligands such as mhp, than two-atom bridging ligands such as pyrazole.

NMR studies of $[M(COD)(xhp)]_2$ complexes (M ≡ Rh, Ir; xhp ≡ hp, mhp, chp) have been reported [119,122], as have molecular weight determinations [124], and

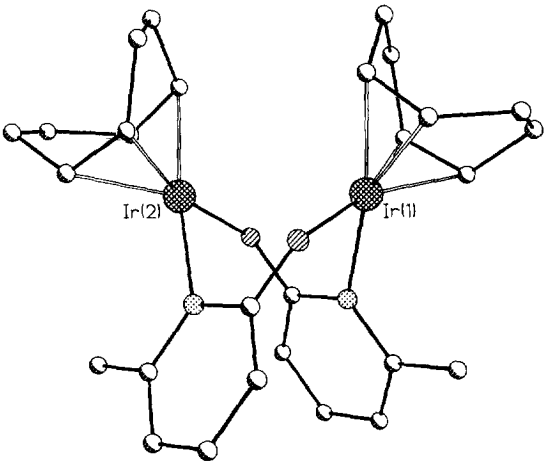

Fig. 19. The structure of $[Ir_2(mhp)_2(COD)_2]$ in the crystal (based on data from ref. 118).

show that the dinuclear structures are maintained in solution. However, the major physical study of these complexes concerns their electronic structure and photochemical and electrochemical properties. Mann and co-workers have examined the excited state properties of these complexes [120] and also their electrochemistry [121].

$[M(diolefin)(xhp)]_2$ complexes have a similar photochemistry to other d^8–d^8 complexes. Two low-energy bands are seen in the electronic absorption spectra at about 20490 and 16950 cm^{-1} for M≡Ir and about 23755 and 20750 cm^{-1} for M≡Rh. These are assigned as transitions from $d\sigma^*$ to $p\sigma$ orbitals, where $d\sigma^*$ is the antibonding orbital derived from the overlap of the d_{z^2} orbitals on each metal and $p\sigma$ is the orbital derived from the overlap of the p_z orbitals. The first absorption band is more intense and assigned to a singlet–singlet transition, while the second weaker, lower energy band is due to a spin-forbidden singlet–triplet transition. The higher energies for the transitions in the rhodium complexes than in the iridium complexes are consistent with a weaker M–M interaction in the former complexes, which is in turn consistent with the longer M–M distance. Two emission bands are also seen for the iridium complexes at about 16500 and 13700 cm^{-1}. These are assigned as the reverse transitions of those responsible for the absorption spectra. Lifetime measurements and quantum yields of phosphorescence are also described [120].

The difference between the absorption and emission band energies in these complexes is considerably greater than the equivalent difference for the pyrazole-bridged complexes. The excited state, where an electron has been excited from the $d\sigma^*$ to the $p\sigma$ orbital, has a formal M–M single bond unlike the ground state where the M–M bond order is zero. Therefore distortion from the ground state structure is likely, and this distortion will be greater for the flexible xhp-bridged structures than for the inflexible pyrazole complexes. Further evidence for this is provided by the crystal structure of the d^7–d^8 complex $[Rh(NBD)(chp)]_2[PF_6]$ [121]. This compound is prepared by oxidation of $[Rh(NBD)(chp)]_2$ with $AgPF_6$. The Rh–Rh distance is much shorter at 2.819(1) Å and the two rhodium atoms remain equivalent. The EPR spectrum of this radical (frozen glass, 130 K, CH_2Cl_2) shows three broad signals at $g=2.08$, 2.21 and 2.25. For the related $[Rh(NBD)(mhp)]_2^+$ complex, the lowest field signal is resolved into a 1:2:1 triplet indicating coupling of the electron to two equivalent ^{103}Rh nuclei [121].

The reactivity of these complexes has also been explored [118,123]. Irradiation or $[Ir(COD)(hp)]_2$ at $\lambda>400$ nm in CCl_4 gives the mononuclear iridium(III) complex $[Ir(COD)(hp)Cl_2]$ [118] (Fig. 20). This contains a chelating hp ligand and the reaction which gives this product is a four-electron oxidation of the dinuclear complex. This is quite unlike the reactions of $[Ir(COD)(pz)]_2$ where two-electron oxidations occur to give d^7–d^7 $[Ir(COD)(pz)Cl]_2$ [127].

The diolefin ligands can be displaced by carbon monoxide to give $[M(CO)_2(hp)]_2$ complexes [123]. The complex with M≡Rh has been structurally characterized and contains the expected pair of bridged square planar metal centres;

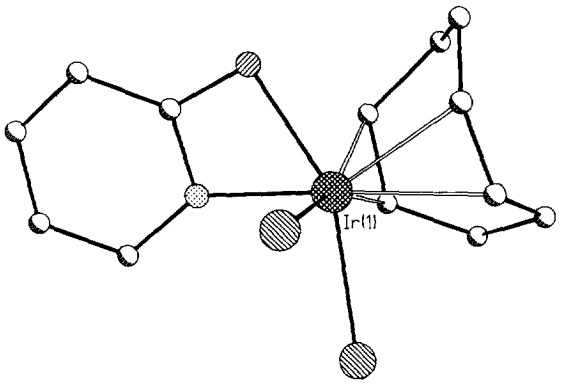

Fig. 20. The structure of $[IrCl_2(hp)(COD)]$ in the crystal (based on data from ref. 118).

however, the hp ligands are oriented head-to-head rather than head-to-tail as in the diolefin compounds (Fig. 21), and the two Rh atoms therefore have dissimilar coordination environments. The Rh–Rh distance is 2.899(2) Å within the dimer unit, and the dimers are stacked so that there is a short intermolecular Rh–Rh contact of 3.410(2) Å. The short intramolecular Rh–Rh distance supports the view that the controlling factor in the diolefin complexes is the steric repulsion between the olefin ligands. The tetracarbonyl complexes can also be prepared directly by reaction of $[Rh(CO)_2(\mu\text{-}Cl)]_2$ with Hhp in the presence of potassium hydroxide under a carbon monoxide atmosphere [123].

If $[Rh(CO)_2(hp)]_2$ is dissolved in a polar solvent, such as methanol, it slowly loses CO and a tetrametallic complex $[Rh_4(hp)_4(\mu\text{-}CO)_2(CO)_4]$ can be isolated [124]. This has a parallelogram of rhodium atoms with each Rh–Rh vector bridged by an hp unit (Fig. 22). In addition, two of these contacts are bridged by carbonyls giving short Rh–Rh contacts of 2.6197(8) Å, while the other Rh–Rh edges are 3.0325(7) Å in length. The loss of CO is reversible; the tetranuclear complex can be converted into the dinuclear complex by the addition of CO in dichloromethane.

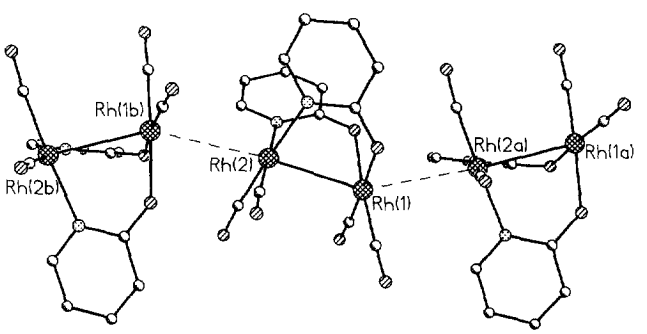

Fig. 21. The stacking of the dimer $[Rh_2(hp)_2(CO)_4]$ in the crystal (based on data from ref. 123).

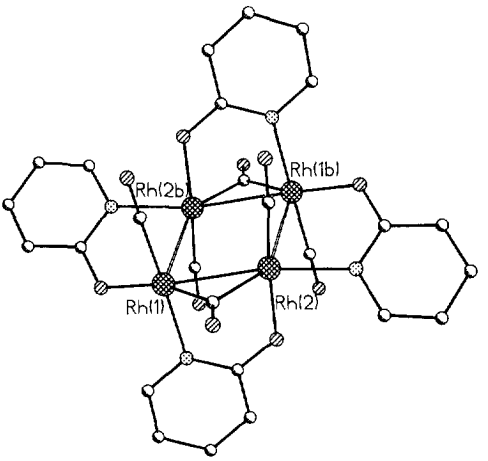

Fig. 22. The tetranuclear compound $[Rh_4(hp)_4(CO)_6]$ in the crystal (based on data from ref. 124).

The CO ligands in $[Rh(CO)_2(hp)]_2$ can be replaced stepwise by PPh_3 to give $[Rh_2(CO)_3(PPh_3)(hp)_2]$ and $[Rh_2(CO)_2(PPh_3)_2(hp)_2]$ [123]. Two of the carbonyls can be replaced to give $[(COD)Rh(hp)_2Rh(CO)_2]$. For each of these complexes, a number of isomers based on the bridged dinuclear structure can be proposed and mixtures are observed [123]. $[Rh(CO)_2(hp)]_2$ also reacts with MeI to give, perhaps unexpectedly, $[RhI(CO)_2(MeCOOC_5H_4N)]$, where $MeCOOC_5H_4N$ is 2-acetoxypyridine [123]. This reaction must involve an initial oxidative addition of MeI to the dinuclear complex, followed by dissociation to a mononuclear comnplex and a CO insertion step. The exact mechanism is unclear. The final product is proposed to be a four-coordinate Rh(I) complex, bound to the pyridine nitrogen of the transformed ligand [123]. The compound was not structurally characterized.

9. THE NICKEL TRIAD

No 2-pyridone complexes of the first-row metal have been reported for this triad, and unlike earlier triads, there are comparatively few molecules reported which contain the $M_2(xhp)_4$ core [128,129]. The vast majority of work has involved dinuclear complexes bridged by only two xhp ligands [3,130–146].

9.1. Dinuclear Pd complexes with four bridging ligands

Five crystallographic determinations have been carried out on compounds of this type; three of these are of different solvates of $[Pd_2(chp)_4]$ [129], while two are of different solvates of $[Pd_2(mhp)_4]$ [128,129]. While this is a limited range of complexes, both the D_{2d} and C_{2h} isomers of the $[M_2(xhp)_4]$ unit are found. Reported physical studies are also limited.

$[Pd_2(mhp)_4]$ was first reported by Clegg et al. in 1982 [128]. As with all other palladium complexes of this type, it was prepared from the reaction of anhydrous palladium acetate with the sodium salt of the ligand in dichloromethane. The unit cell parameters and space group are identical with $[Rh_2(mhp)_4]$. The compound has the expected D_{2d} geometry of the ligands with a Pd–Pd contact of 2.546(1) Å, which is 0.187 Å longer than the Rh–Rh bond in the homologous compound. The electronic configuration of the metals indicates that no net metal–metal bond is expected in $[Pd_2(mhp)_4]$. Unfortunately, the lack of volatility of the complex is such that photoelectron spectroscopy has not been able to confirm this prediction [128].

The crystal structures of three different solvates of $[Pd_2(chp)_4]$ have also been reported [129]. In each case, the D_{2d} isomer is found with Pd–Pd contacts of between 2.563(1) and 2.570(1) Å. In the same paper, a second structural determination was carried out on a compound with the formula $[Pd_2(mhp)_4]$. On this occasion, the compound crystallized with five dinuclear molecules in the asymmetric unit. Four of these molecules have the expected approximate D_{2d} symmetry; however, the fifth molecule lies on an inversion centre and has approximate C_{2h} symmetry (Fig. 23), i.e. although two nitrogens and two oxygens from mhp are attached to each metal, the arrangement of like donor atoms is cis about each metal rather than trans. This is the second example of this geometry found for $[M_2(xhp)_4]$ complexes, the other being $[Re_2(hp)_4Cl_2]$ [76]. The Pd–Pd contacts average 2.547(6) Å for the D_{2d} isomers and are insignificantly longer at 2.559(3) Å in the C_{2h} form.

9.2. *Dinuclear Pd and Pt complexes with two bridging ligands*

This work has been carried out by three research groups, i.e. those led by Lippard, Cotton and Matsumato. The reports from Lippard's group [3,38,130–140]

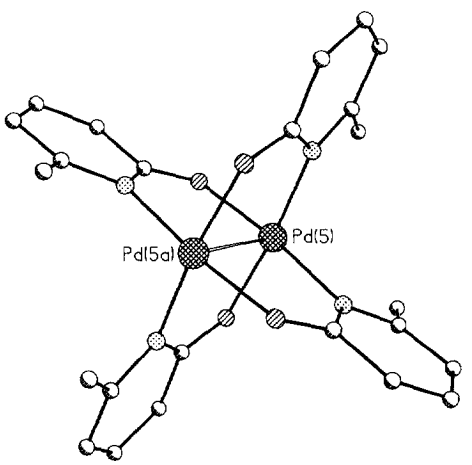

Fig. 23. The structure of the C_{2h} isomer of $[Pd_2(mhp)_4]$ in the crystal (based on data from ref. 129).

deal with the use of 2-pyridone as a model for pyrimidine nucleobases such as uracil or thymine. The work from Cotton and co-workers [141–143] extends their study of metal–metal bonding. Matsumato's group [144,145] has investigated palladium complexes similar to the platinum complexes described by Lippard.

The syntheses of these complexes fall into two groups. The Pt(II), Pd(II) and Pt complexes with the metals in non-integer oxidation states are prepared from *cis*-$[Pt(NH_3)_2Cl_2]$ or $[M(en)X_2]$ ($M \equiv Pd$, Pt; $X \equiv Cl$, I) (en = 1,2-diaminoethane) in water, and isolated by the judicious control of pH. Some of the syntheses require the addition of silver nitrate before the addition of Hhp [3,134], some require the addition of silver nitrate after the addition of Hhp and NaOH [144,145], and mononuclear complexes can be prepared without the addition of a silver salt to precipitate halides [38]. Several of these reactions give multiple products [131]. The Pt(III) complexes featuring NH_3 or en as ligands are prepared in water by the oxidation of Pt(II) complexes with nitric acid [135,136]. If a halide is present in the Pt(III) complex, it is added before oxidation as the sodium salt [136].

The tetramethyl platinum(III) complexes are prepared by the reaction of $[Pt_2(CH_3)_4(SEt_2)_2]$ with the silver salt of the requisite xhp ligand [141–143]. This reaction involves not only ligand transfer from silver to platinum, but also oxidation of Pt^{2+} to Pt^{3+} by silver which is reduced and precipitates as a colloid. The pyridine adducts [141,142] are prepared from the crude SEt_2 adducts.

The structures are listed in Table 7. All feature M_2 units bridged by two xhp ligands arranged cis on each metal. There are two possible isomers for this arrangement: a head-to-head (HH) isomer where both xhp oxygens are attached to one metal and both xhp nitrogens to the second, and a head-to-tail (HT) isomer in which both metals are bound to one oxygen and one nitrogen from the bridging xhp ligands. The factors which decide which isomer is preferred appear to be finely balanced. Steric factors suggest that, if one axial ligand is to be attached to the metal, the HH isomer should be preferred, while for pyridones with small substituents in the 6-position, i.e. hp and fhp, two axial ligands can be attached to the HT isomer. For the HT isomer $[Pt_2(CH_3)_4(fhp)_2(py)_2]$ (Fig. 24), one of the axial pyridine (py) ligands can be removed, causing rearrangement to the HH isomer $[Pt_2(CH_3)_4(fhp)_2(py)]$ (Fig. 25) [142].

As with the Rh_2^{4+} complexes described above (Section 8.2), dimerization can be an alternative to axial ligation. This has so far been reported only for the HH isomers of the complexes containing ammonia and 1,2-diaminoethane, and hydrogen bonding between the exocyclic oxygen of the pyridone ligands in one dimer and the amine ligands in the second must contribute significantly to the stability of these dimers of dimers. Unlike the Rh_2^{4+} complexes, the axial position of each platinum is occupied by the platinum in the neighbouring dimer, rather than a pyridone oxygen (Fig. 26), giving an intermolecular Pt–Pt contact of less than 3.3 Å.

For the Pt(II) complexes, there is no net metal–metal bond as the electronic configuration is $\sigma^2\pi^4\delta^2\delta^{*2}\pi^{*4}\sigma^{*2}$. For the Pt(III) complexes, there is a net single

TABLE 7

Structurally characterized Pt and Pd complexes with two bridging pyridone ligands

Formula	Oxidation state	Isomer	No. of axial ligands	Pt–Pt bond length (Å)	Reference
$[Pt_2(NH_3)_4(hp)_2](NO_3)_2$	2	HT	0	2.8981(5)	137
$[Pt_2(NH_3)_4(hp)_2]_2(NO_3)_4$	2	HH	1[a]	2.8767(7), 3.1294(4)[b]	137
$[Pt_2(en)_2(hp)_2]_2(NO_3)_4$	2	HH	1[a]	2.992(1), 3.236(1)[b]	134
$[Pt_2(en)_2(hp)_2]_2(NO_3)_4$	2	HH	1[a]	2.981(1), 3.220(1)[b]	145
$[Pt_2(NH_3)_4(hp)_2]_2(NO_3)_5$	2.25	HH	1[a]	2.7745(4), 2.8770(5)[b]	130
$[Pt_2(en)_2(hp)_2]_2(NO_3)_5$	2.25	HH	1[a]	2.8296(5), 2.9158(5)[b]	140
$[Pt_2(NH_3)_4(hp)_2(NO_3)(H_2O)](NO_3)_3$	3	HT	2	2.5401(5)	135
$[Pt_2(NH_3)_4(hp)_2(NO_3)_2][NO_3]_2$	3	HT	2	2.5468(8)	135
$[Pt_2(NH_3)_4(hp)_2(NO_2)_2](NO_3)_2$	3	HT	2	2.576(1)	136
$[Pt_2(NH_3)_4(hp)_2Cl_2](NO_3)_2$	3	HT	2	2.568(1)	136
$[Pt_2(NH_3)_4(hp)_2Br_2](NO_3)_2$	3	HH	2	2.582(1)	136
$[Pt_2(en)_2(hp)_2(NO_2)(NO_3)](NO_3)_2$	3	HH	2	2.6382(6)	139
$[Pt_2(CH_3)_4(hp)_2(py)_2]$	3	HT	2	2.550(1)	141
$[Pt_2(CH_3)_4(fhp)_2(py)_2]$	3	HT	2	2.551(2)	141
$[Pt_2(CH_3)_4(chp)_2(py)]$	3	HH	1	2.543(1)	141
$[Pt_2(CH_3)_4(mhp)_2(py)]$	3	HH	1	2.545(1)	141
$[Pt_2(CH_3)_4(hp)_2(py)]$	3	HH	1	2.556(1)	142
$[Pt_2(CH_3)_4(fhp)_2(py)]$	3	HH	1	2.554(1)	142
$[Pt_2(CH_3)_4(bhp)_2(py)]$	3	HH	1	2.551(1)	142
$[Pt_2(CH_3)_4(hp)_2(SEt_2)]$	3	HH	1	2.568(1)	143
$[Pt_2(CH_3)_4(fhp)_2(SEt_2)]$	3	HH	1	2.571(1)	143
$[Pt_2(CH_3)_4(mhp)_2(SEt_2)]$	3	HH	1	2.561(1)	143

[a] The molecule is a dimer.

[b] The second M–M distance is the interdimer bond.

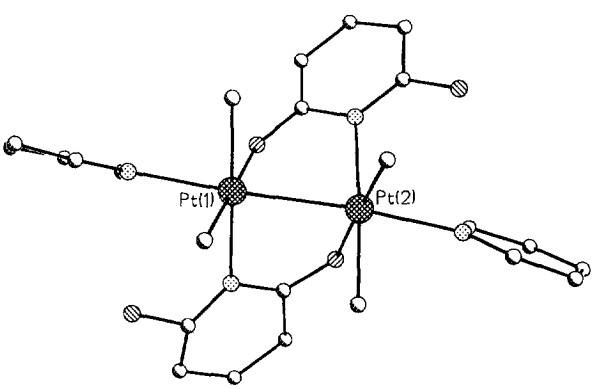

Fig. 24. The structure of the head-to-tail complex $[Pt_2Me_4(fhp)_2(py)_2]$ in the crystal (based on data from ref. 142).

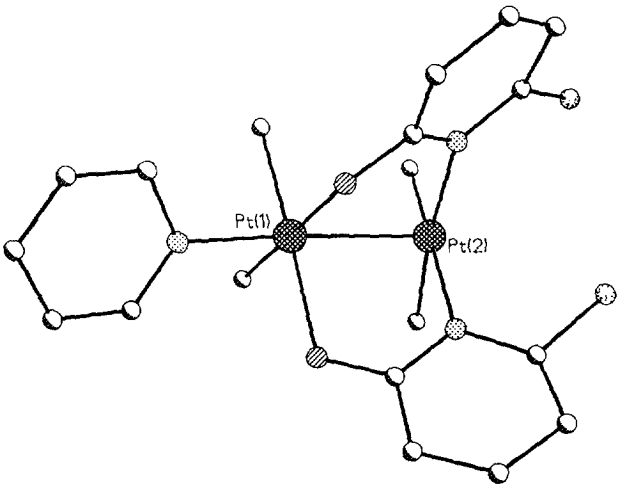

Fig. 25. The structure of the head-to-head complex $[Pt_2Me_4(fhp)_2(py)]$ in the crystal (based on data from ref. 142).

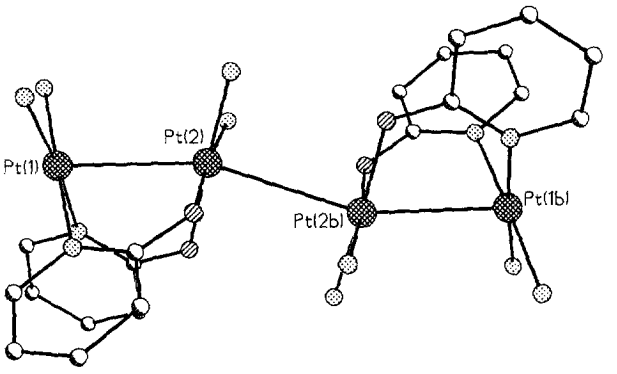

Fig. 26. The structure of the tetranuclear "platinum blue" cation $[Pt_2(NH_3)_4(hp)_2]_2^{5+}$ in the crystal (based on data from ref. 130).

bond. This is reflected in the much shorter bond lengths for the Pt(III) complexes compared with the equivalent Pt(II) complexes, e.g. the average bond length in $[Pt_2(NH_3)_4(hp)_2XX']^{2+}$ complexes is 2.563 Å, while in $[Pt_2(NH_3)_4(hp)_2]^{2+}$ the bond length is 2.898 Å. This shortening of the M–M distance is reminiscent of that observed for $[Rh_2(NBD)_2(chp)_2]$ on oxidation to $[Rh_2(NBD)_2(chp)_2]^+$ [121], where removal of one electron from a σ^* orbital reduces the M–M contact by 0.221 Å. Within the $[Pt_2(NH_3)_4(hp)_2XX']^{2+}$ complexes, the Pt–Pt bond appears to correlate with the π-donating ability of X and X'. If $X \equiv H_2O$ and $X' \equiv NO_3^-$, the bond length is 2.540 Å, while for $X \equiv X' \equiv Br^-$, the bond lengthens to 2.582 Å. All the tetramethyl platinum(III) complexes fall within this 0.042 Å range, which suggests

minimal influence from the presence of ammonia or methyl ligands. The only Pt^{3+} complex with a longer Pt–Pt bond, 2.638 Å is $[Pt_2(en)_2(hp)_2(NO_2)(NO_3)]^{2+}$ which is presumably caused by steric repulsion between the en ligands on the two platinum atoms. In the $[Pt_2(CH_3)_4(xhp)_2(py)_n]$ complexes, neither the identity of xhp nor the number of axial pyridine ligands affects the Pt–Pt bond length significantly. For the two complexes containing a platinum in an oxidation state of 2.25, the intradimer Pt–Pt bond lengths are 2.775 and 2.830 Å, predictably intermediate between the lengths in the +2 and +3 oxidation state complexes.

In addition to these dimeric complexes, three mononuclear platinum complexes of pyridones were crystallographically characterized by Hollis and Lippard [38]. These are the Pt(II) complexes *cis*-$[Pt(NH_3)_2(Hhp)_2Cl_2]$ and *cis*-$[Pt(NH_3)_2(Hhp)Cl](NO_3)$, and the Pt(IV) complex mer-$[Pt(NH_3)_2(hp)Cl_3]$. In all cases, the pyridone, whether protonated or not, is bound via the ring nitrogen to Pt. For Hhp this is unlike the behaviour in complexes of first-row metals, where it binds through the oxygen atom, and indicates that the ligand is bound as the pyridinol tautomer.

9.3. *Physical studies*

The work reported by Lippard and co-workers derives its chief motivation from its relevance to the binding of the anti-cancer drug *cis*-$[Pt(NH_3)_2Cl_2]$ to pyrimidine nucleobases. Unfortunately, reaction of *cis*-$[Pt(NH_3)_2Cl_2]$ with molecules such as uracil or thymine leads to ill-defined, non-crystalline dark blue materials which are difficult to characterize. Use of a ligand with similar, but more restricted, numbers of donor sites, such as 2-pyridone, allows isolation and full characterization of relevant platinum complexes. Related work has used 1-methyluracil and 1-methylthymine, which restricts coordination of the ligands by blocking one of the pyrimidine nitrogens [146]. The chief thrust of the physical studies on the platinum–amine–pyridone complexes has therefore been to use these models to understand the nature of the "platinum blues" formed when *cis*-$[Pt(NH_3)_2Cl_2]$ is reacted with uracils.

The first compound reported in this class contained the tetranuclear $[Pt_2(NH_3)_4(hp)_2]_2^{5+}$ cation [3,130]. This compound gives dark blue crystals and contains platinum in a non-integer oxidation state. EPR studies of this complex as a single crystal [130] give the three principle components of the g tensor as $g_{xx}=2.307$, $g_{yy}=2.455$ and $g_{zz}=1.975$. No hyperfine interactions were observed in the single crystal spectra. The z axis is taken to be along the Pt_4 chain and the values of the g tensor indicate a d_{z^2} hole state. The EPR spectra of a frozen glass [147] are consistent with the same g tensor, but extensive hyperfine coupling to ^{195}Pt nuclei is observed. The number of hyperfine lines is consistent with the unpaired electron being delocalized over all four platinum nuclei. The effective magnetic

moment shows the presence of one unpaired electron per tetranuclear unit [130]. All these observations suggest a formal platinum oxidation state of 2.25.

The electronic spectrum of $[Pt_2(NH_3)_4(hp)_2]_2^{5+}$ in aqueous solution shows a broad absorption band centred at 14 705 cm^{-1}. The extinction coefficient for this band is dependent on time and the presence of a variety of anions such as nitrate, perchlorate, chloride and acetate [130]. Oxidative titration of $[Pt_2(NH_3)_4(hp)_2]_2^{5+}$ with cerium(IV) shows an end point with 0.77 equivalents of oxidant per platinum. This indicates that the platinum atoms are being oxidized from $Pt^{2.25+}$ to Pt^{3+}, which is in agreement with the observed stability of Pt(III) dimers of this ligand system.

As $[Pt_2(NH_3)_4(hp)_2]_2^{5+}$ was the first "platinum blue" to be structurally characterized, the comparison of the physical properties of this compound with those of amorphous platinum blues led to important insights into the structures of all these materials. Extended X-ray absorption fine structure (EXAFS) studies [148] on a platinum uridine complex showed that the Pt–Pt separations were similar to those observed in the structurally characterized compound. An X-ray photoelectron spectroscopy (XPS) study [149] revealed that several platinum blues had the same electronic structure as $[Pt_2(NH_3)_4(hp)_2]_2^{5+}$. Taken together, these two results suggest that all platinum blues are oligomeric, contain mixed-oxidation state amidate-bridged platinums, and have short intermolecular Pt–Pt contacts. More recent structural studies [140,150,151] of platinum blues have tended to confirm this supposition. SCF-X_α calculations, combined with polarized single crystal optical spectroscopy [140,152], have also led to the assignment of the absorption band responsible for the blue colour of $[Pt_2(NH)_3)_4(hp)_2]_2^{5+}$. The transition involves the two central Pt atoms of the tetranuclear cation, and is between a Pt–Pt σ-bonding and σ^*-antibonding orbital [152]. This again indicates that all "platinum blues" are likely to be oligomeric.

The Pt(II) and Pt(III) amine complexes have also been the subject of a number of physical studies. These include ^{195}Pt NMR studies of both Pt(II) [138] and Pt(III) [139] dimers. The chemical shift range for the Pt(II) complexes is between -1308 and -2495 ppm, while for the Pt(III) complexes the range is between -1141 and $+541$ ppm. The $^1J_{Pt-Pt}$ coupling constant is unresolved in the Pt(II) complexes, but is around 6850 Hz for the Pt(III) complex reported.

A study of the electrochemistry of three of these complexes has been reported [135]. The HT Pt(II) dimer $[Pt_2(NH_3)_4(hp)_2](NO_3)_2$ shows a quasi-reversible two-electron oxidation with $E_{1/2} = +0.62$ V. Exhaustive electrolysis of this complex at $+0.85$ V results in a net loss of 0.95 electrons per Pt, and gives a solution which has an electrochemistry identical with that of the HT Pt(III) dimer $[Pt_2(NH_3)_4(hp)_2(NO_3)_2](NO_3)_2$, i.e. a quasi-reversible two-electron reduction at $+0.62$ V. The HH Pt(III) dimer $[Pt_2(NH_3)_4(hp)_2(H_2O)(NO_3)](NO_3)_3$ also undergoes a two-electron reduction at $E_{1/2} = +0.63$ V; however, exhaustive reductive electrolysis of this complex is accompanied by a series of colour changes, from orange

to green to blue to colourless. The blue colour is most intense after the addition of 0.75 electrons per platinum, which suggests that a tetranuclear mixed-valent platinum complex is formed as an intermediate during the reduction of the Pt(III) dimer to a Pt(II) dimer. The tetranuclear Pt complexes have only been observed for HH isomers; therefore this observation is in agreement with crystallographic studies.

No physical studies have been reported for the tetramethyl Pt(III) dimers, and only ^{13}C and ^{1}H–^{13}C COSY NMR studies of the palladium dimers [145]. The NMR studies indicate that the HH isomer found in the crystal isomerizes in solution to give a mixture of the HH and HT isomers.

10. THE COPPER TRIAD

This triad provides the exception to the rule that much more work has been done on the second- and third-row metal complexes of 2-pyridones than on the first-row metal. For Group 12 a large body of work exists for copper; no structures have been reported for silver compounds of these ligands, although silver complexes have been used as reagents for synthesizing metal complexes of pyridones; only one gold complex has been structurally characterized.

10.1. Copper complexes

The copper complexes reported show a structural diversity quite unlike that of other metals. Although dimeric compounds have been reported, there are also reports of tetranuclear, hexanuclear and heptanuclear homoleptic complexes of these ligands and several further heteroleptic complexes. There is also an expanding body of work on heterometallic complexes of pyridones which feature copper as one of the metals present.

The earliest report of a copper complex of a 2-pyridone ligand was the mononuclear complex of the protonated parent ligand $[Cu(Hhp)_6][ClO_4]_2$ [46]. It was later characterized by X-ray crystallography [35]. The synthesis is from copper(II) perchlorate and Hhp in the presence of a dehydrating agent, and the structure contains copper coordinated to six oxygens from the Hhp ligands which are present in the pyridone tautomeric form. The coordination geometry shows the expected tetragonal elongation from octahedral.

Other copper complexes of Hhp and other protonated pyridones have included compounds in which two 2-pyridone ligands are bound via the oxygen in the axial position of copper carboxylate dimers [22,153]. The room temperature magnetic moments of a series of copper benzoate complexes with various 2-pyridones have been reported [22], and their magnetic properties seem rather insensitive to the pyridone derivative present. The crystal structure of $[Cu_2(O_2CCH_3)_4(Hhp)_2]$ has been solved [153].

One further copper complex of Hhp has been reported, $[Cu_2(Hhp)_4Cl_4]$ [154]

(Fig. 27). The two copper atoms are five coordinate and are bridged by two μ_2-exocyclic oxygens from Hhp with a Cu–Cu distance of 3.4448(11) Å. The remainder of the copper coordination spheres are made up of two chlorides and one oxygen from a further Hhp ligand. Thus the complex contains both bridging Hhp and terminal Hhp ligands. The protic hydrogens were not located in the structural determination, but it seems clear that the ligands are coordinated as the pyridone tautomer.

The first reported dimeric copper complexes of pyridones [20,155,156] were synthesized by refluxing a mixture of the required ligand and copper hydroxide in dimethylformamide (DMF) [20] or DMSO [155]. Unusually, the ligands used were the 3-ethyl, 3-methyl and 4-methyl derivatives [20], in addition to hp itself [155,156]. Given these ligands and the highly polar solvents used, it is not surprising that the resulting, highly insoluble compounds have the formula $[Cu_2(xhp)_4(sol)_2]$ with solvents in the axial positions of the copper (Fig. 28). The isomer has the D_{2d} arrangement of ligands, as found for the dimers of Group 6 metals (see Section 5.2). Copper dimers with further derivatives, including 3-chp, 3-bhp, 3-NO_2hp, 5-chp and 5-NO_2hp, were also synthesized in a similar manner [21], and the magnetic properties of these complexes have been studied. The two copper atoms are antiferromagnetically coupled, giving a singlet ground state and a triplet excited state. Application of the Bleaney–Bowers equation [157] gives the energy gap, $2J$, as between 395 and 405 cm^{-1} for the dimers containing alkylated pyridones, 360–365 cm^{-1} for the dimers of hp, and 314 cm^{-1} for the dimer with 3-NO_2hp ligands. The room temperature magnetic moment can be correlated with pK_a for the protonation of oxygen in the neutral ligand [21]. An EPR study of the dimers with 3-Ethp and 3-Mehp has also been reported [158]. Compared with similar dimeric copper complexes, e.g. of acetate [159] or adenine [160], the zero-field splitting parameters are midway

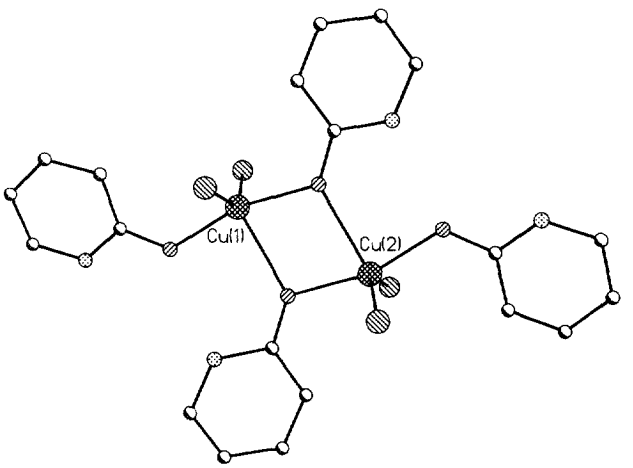

Fig. 27. The structure of $[Cu_2(Hhp)_4Cl_4]$ in the crystal (based on data from ref. 154).

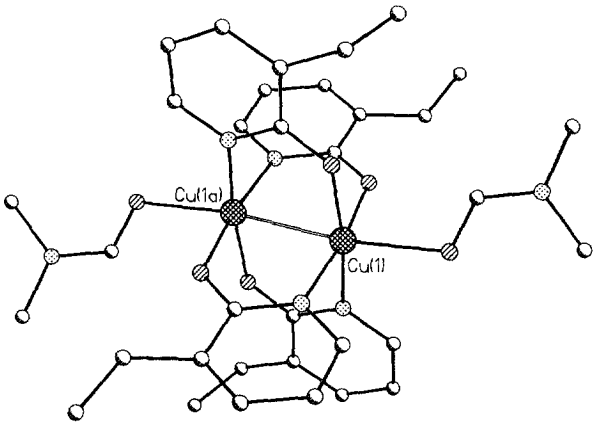

Fig. 28. The structure of $[Cu_2(3\text{-Ethp})_4(DMF)_2]$ in the crystal (based on data from ref. 20).

between those for complexes with exclusively oxygen and exclusively nitrogen donors, while the exchange coupling constants are generally larger.

A further, heteroleptic dimer of hp has been reported by Nishida et al. [161]. This is the planar complex $Cu(hp)(C_{10}H_{14}N_2O_3)$ (Fig. 29). Each copper is four coordinate, bound to the central μ_2-oxygen of the pentadentate ligand, and to two further donor atoms from this ligand, but to either the oxygen or nitrogen of hp. The copper–copper distance is 3.25 Å.

A dimeric copper complex of chp has also been reported [162]. The presence of chloro substituents in the 6-position prevents the axial coordination of the solvent and this possibly leads to a somewhat shorter Cu–Cu contact of 2.4989(11) Å than in the previously reported dimers, e.g. 2.550(1) Å for $[Cu_2(3\text{-Ethp})_4(DMF)_2]$ [20].

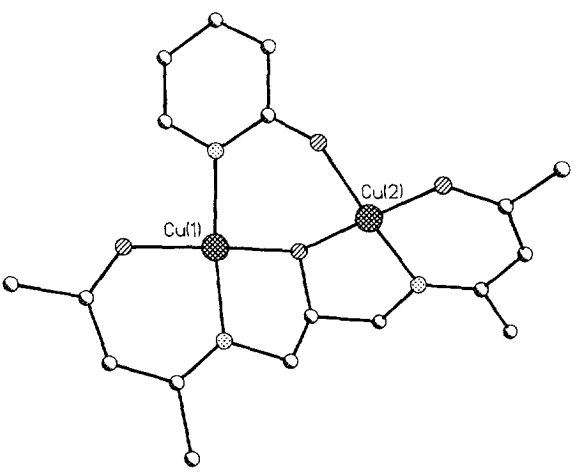

Fig. 29. The structure of $[Cu_2(hp)(C_{10}H_{14}N_2O_3)]$ in the crystal (based on data from ref. 161).

This complex is much more soluble than the previously reported copper dimers. $[Cu_2(chp)_4]$ is EPR silent at 77 K in CH_2Cl_2, and has a magnetic moment of $1.58\mu_B$ per formula unit at room temperature. This magnetic moment is higher than those reported for complexes of other derivatives, e.g. $1.41\mu_B$ for $[Cu_2(3\text{-}NO_2hp)_4(DMF)_2]$. All the dimeric compounds reported are intensely coloured (dark green for all except $[Cu_2(chp)_4]$ which is dark red), but no thorough investigation of the electronic spectroscopy of these compounds has been reported. This is possibly related to the generally low solubility of these complexes.

$[Cu_2(chp)_4]$ was synthesized by reaction of hydrated copper nitrate with K(chp) in the solid state, followed by crystallization from CH_2Cl_2–ether. A similar reaction using K(mhp) gave a novel hexanuclear copper complex, $[Cu_6Na(mhp)_{12}][NO_3]$ [8] (Fig. 30). The presence of a sodium ion can be accounted for by an impurity in K(mhp). The arrangement of the six coppers in the cation resembles a "Star of David". The coppers are each four coordinate and bound to two nitrogen and two oxygen donors from mhp. For three of the copper atoms, these donors are arranged in a cis fashion, while for the other three atoms they are arranged trans. The oxygens attached in a cis fashion form a hexadentate cavity in which the sodium ion is found. This makes the compound a structural analogue of a crown ether. Mass spectroscopy indicates that the structure is quite robust as peaks are seen for the parent ion in addition to fragments for $[Cu_nNa(mhp)_{2n}]^+$ ($n = 1, 2, 3, 4, 5$). Proton and ^{23}Na NMR indicate that the structure is retained in chlorinated hydrocarbons [10].

Reaction of $[Cu_6Na(mhp)_{12}][NO_3]$ with lead nitrate leads to the formation of a heptanuclear copper complex $[Cu_7(mhp)_{12}][Pb(NO_3)_4]$ [10]. The cation in this salt is superimposable with that in $[Cu_6Na(mhp)_{12}][NO_3]$ except that the central sodium has been replaced by a further copper. The nature of this reaction is

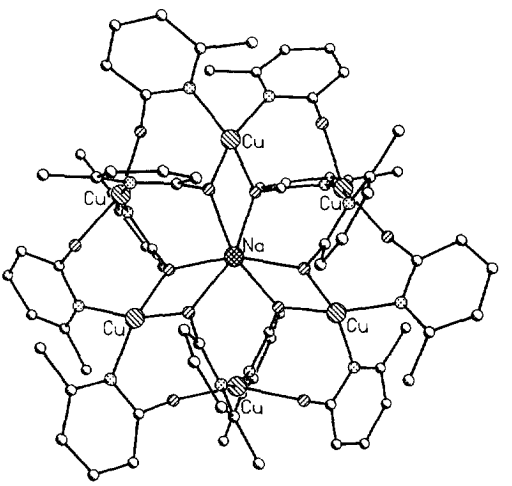

Fig. 30. The structure of the hexanuclear cation $[Cu_6Na(mhp)_{12}]^+$ in the crystal (based on data from ref. 8).

unclear. Mass spectroscopy shows peaks for both the parent ion and for $[Cu_{n+1}(mhp)_{2n}]^+$ fragments [10]; however, proton NMR shows that the complex dissociates in solution.

The reactivity of $[Cu_2(chp)_4]$ has been explored [55]. It is soluble in chlorinated hydrocarbons, giving a deep red solution, but the addition of any coordinating solvents, such as methanol, ethanol, DMF or pyridine, leads to a colour change to green, and EPR spectroscopy of these solutions suggests the presence of mononuclear copper complexes which are presumably $[Cu(chp)_2(sol)_2]$ and related compounds. From methanol–dichloromethane purple crystals of $[Cu_4(chp)_4(OCH_3)_4]$ can be grown [55]. This structure contains a parallelogram of copper atoms with alternate sides bridged by two methoxides or two chp ligands. The Cu–Cu distances within the parallelogram are 2.966(1) and 2.811(1) Å for the methoxide- and chp-bridged vectors respectively. The copper atoms are four coordinate, bound to two μ_2-oxygens from methoxide, one chp oxygen and one chp nitrogen. The coordination geometries about each copper are close to square planar with the only significant distortion being an acute angle of about 76° between the two methoxide oxygens. The coordination planes of the two coppers bridged by μ_2-oxygens from methoxide are at an angle of 20.4° to each other.

$[Cu_2(chp)_4]$ also reacts with 1,2-ethanediol to give a one-dimensional polymer with the formula $[Cu_3(chp)_4(OCH_2CH_2OH)_2]_n$ (Fig. 31) [55]. This contains two distinct copper coordination sites. The first is similar to the copper site in $[Cu_4(chp)_4(OCH_3)_4]$ with the copper bound to two deprotonated μ_2-oxygen from diol ligands, one oxygen from chp and one nitrogen from chp. The chp ligands bridge onto the second copper which sits on an inversion centre and is coordinated to a trans array of two oxygens and two nitrogens from chp ligands.

Two further copper chp complexes have been reported. Both can be synthesized directly from simple copper salts, e.g. copper acetate, or via $[Cu_2(chp)_4]$ [55]. Reaction of $[Cu_2(chp)_4]$ with bipyridyl leads to a new dimeric complex, $[Cu_2(chp)_4(bipy)_2]$. This contains two five-coordinate copper centres bridged by the μ_2-oxygens from two chp units. This is reminiscent of the bridging in the only structurally characterized vanadium complex of these ligands, but differs in that the

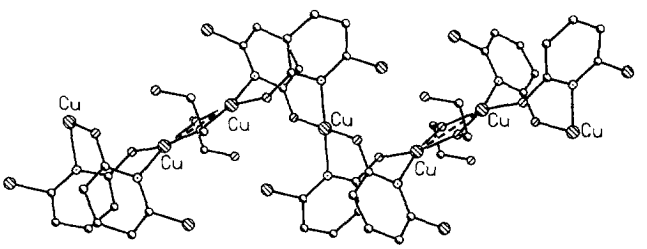

Fig. 31. The structure of the polymeric complex $[Cu_3(chp)_4(OCH_2CH_2OH)_2]_n$ in the crystal (based on data from ref. 55).

chp remains deprotonated. The complex also contains two terminal, deprotonated chp ligands.

$[Cu_2(chp)_4]$ reacts with copper acetate to produce an unusual octameric complex, $[Cu_8(O)_2(OAc)_4(chp)_8]$ (Fig. 32) [55]. This compound contains an oxo-centred edge-sharing bitetrahedron of coppers encapsulated by two $[Cu(chp)_4]^{2-}$ units. The $Cu_6(O)_2$ core appears to be the first example of such a unit.

Reaction of $[Cu(O_2CCF_3)]$ in ethanol with Na(mhp) gives an interesting tetranuclear complex $[Cu(mhp)]_4$ (Fig. 33) [163]. This contains a puckered square of Cu(I) atoms with each edge bridged by one mhp ligand. Each copper is coordinated to one N and one O from an mhp unit, with bond angles of about 170°. The Cu–Cu distances within this square average 2.678 ± 0.022 Å. These contacts represent weak Cu(I)–Cu(I) interactions, which are by no means unusual. $[Cu(mhp)]_4$ remains the only structurally characterized copper(I) complex of these ligands.

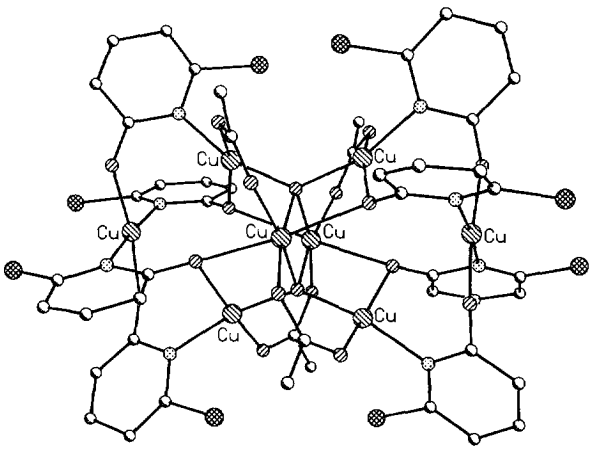

Fig. 32. The structure of the octanuclear complex $[Cu_8(O)_2(chp)_8(OAc)_4]$ in the crystal (based on data from ref. 55).

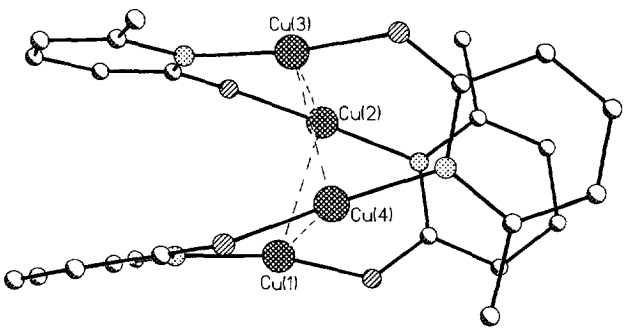

Fig. 33. The structure of the tetranuclear complex $[Cu_4(mhp)_4]$ in the crystal (based on data from ref. 163).

10.2 Silver complexes

Silver salts of hp, bhp, chp, fhp and mhp can be synthesized from silver nitrate and the sodium salt of the ligand in water, from which Ag(xhp) precipitates immediately [141,142]. They are off-white in colour and moderately light sensitive. No further characterization of these complexes has been reported, which is perhaps surprising, especially given the attractive structure of the only reported copper(I) complex of 2-pyridones. These silver salts have been used as a reactant in the preparation of platinum dimers bridged by 2-pyridone ligands [141–143] (see Section 9.2).

10.3 Gold complexes

A series of gold phosphine complexes of 2-pyridones has been reported [164]. These include $Au(PPh_3)$(xhp) complexes, where xhp ≡ 5-chloro- and 3-nitro-2-pyridone in addition to mhp, and $Au(PR_3)$(hp) complexes, where R ≡ Ph, ^{t}Bu, cyclohexyl and 1-naphthyl. The aim of this work was to isolate C-metallated pyridones; however, all the compounds made contain gold attached to the nitrogen of the pyridone ligand. This implies that the pyridone tautomer is present, rather than the pyridonol form. This is not surprising given the preference of gold for nitrogen rather than oxygen donors and the pyridone derivatives chosen. Surprisingly, no experiments using chp, which might conceivably support the pyridonol form, have been reported. Proton NMR spectra of the various compounds synthesized have also been reported [164], but only one ^{31}P NMR chemical shift.

10.4 Heterometallic complexes featuring copper

Cotton and Hansen [71] reported the first heterometallic complex of pyridones in 1978 with the synthesis of $MoW(mhp)_4$. This complex is described in Section 5.5. The use of pyridones to bridge quite different metals dates from 1989, and a report by Goodgame et al. [5]. This work has been followed up by two groups, our own and that led by Wang.

This work was inspired by the discovery of high-temperature superconducting oxides which contained copper and a mixture of other s-, p- or f-block metals [165]. It was hoped that by using an ambidentate bridging ligand, such as 2-pyridone, it would be possible to synthesize molecular species which contain both copper and a second metal. These molecular species could then be used to study the unusual metal–metal interactions which give rise to the unusual properties of the oxides, or possibly as precursors for the synthesis of the oxides themselves.

The first compounds reported used hp as a ligand and had a metal core of formula Cu_4Ln_2 [5]. They were made from copper hydroxide, Hhp and a lanthanoid nitrate in methanol. The synthesis of complexes containing the same metal core has

since been improved [7] by using K(hp), plus copper and lanthanoid nitrates in methanol. Other synthetic procedures have involved the use of copper methoxide instead of copper hydroxide [6,166], and the isolation of copper pyridone complexes before further reaction with lanthanoid salts [8,162,167]. These synthetic procedures have led to a considerable number of copper lanthanoid complexes, and a smaller number of copper Group 2 complexes; these are listed in Table 8.

The structures of these compounds are complex; even describing the metal core can be difficult. So far, none of the compounds contains fewer copper atoms than atoms of the second metal. Whether this observation is anything more than a coincidence is doubtful; however, it undoubtedly limits the usefulness of the complexes as precursors of mixed-metal oxides, as decomposition products frequently contain high mole ratios of copper(II) oxide.

Three complexes which all contain a 1:1 ratio of Cu:M have been structurally characterized. Each has a quite different arrangement of metals. The first is a comparatively simple complex containing a central $Cu_2(OMe)_2(chp)_4$ unit which bridges between two Yb^{3+} ions (Fig. 34) [162]. The nitrogens of the chp ligands are bound to copper, and the oxygens bind to ytterbium. This is the normal arrangement for the ligands in these mixed-metal complexes.

The second 1:1 compound characterized contains two coppers and two lanthanums [167], but the arrangement is utterly different to that in the Cu_2Yb_2 complex

TABLE 8

Structurally characterized mixed-metal complexes containing copper

M	Cu:M ratio	Formula[a]	Reference
Yb	1:1	$Cu_2Yb_2(chp)_4(OMe)_2(NO_3)_4(HOMe)_4$	162
La	1:1	$Cu_2La_2(chp)_8(Hchp)_2(NO_3)_2$	167
La	1:1	$[Cu_4La_4(hp)_8(Hhp)_8(ClO_4)_2(NO_3)_2(OH)_4(CH_3O)_2][ClO_4]_2$	7
La	3:2	$[Cu_{12}La_8(OH)_{24}(Hmhp)_{13}(NO_3)_{22}(H_2O)_6][NO_3]_2$	8
Gd	2:1	$Cu_4Gd_2(hp)_8(Hhp)_4(OH)_2(NO_3)_4(H_2O)_2$	5
Dy	2:1	$Cu_4Dy_2(hp)_8(Hhp)_4(OH)_2(NO_3)_4(H_2O_2$	5
Gd	2:1	$[Cu_4Gd_2(hp)_8(Hhp)_4Cl_4(H_2O)_4].2Cl$	7
La	3:1	$Cu_3La(chp)_5(OMe)(NO_3)_3(HOMe)_2$	167
La	3:1	$Cu_3La(chp)_8(NO_3)(HOEt)$	167
Mg	3:1	$Cu_3Mg(chp)_6(Hchp)_2(NO_3)_2$	10
Ba	4:1	$BaCu_4(hp)_4(bdmap)_4(O_2CCF_3)_2$[b]	9
Ba	4:1	$BaCu_4(hp)_4(deae)_4(O_2CCF_3)_2$[c]	9
Y	4:1	$Cu_8Y_2(O)_2(hp)_{12}(Cl)_2(NO_3)_4(H_2O)_2$	166
Nd	4:1	$Cu_8Nd_2(O)_2(hp)_{12}(Cl)_2(OCH_3)_4(H_2O)_2$	166

[a] Lattice solvent not included.

[b] bdmapH, 1,3-bis(dimethylamino)-2-propanol.

[c] deaeH, 2-(diethylamino)ethanol.

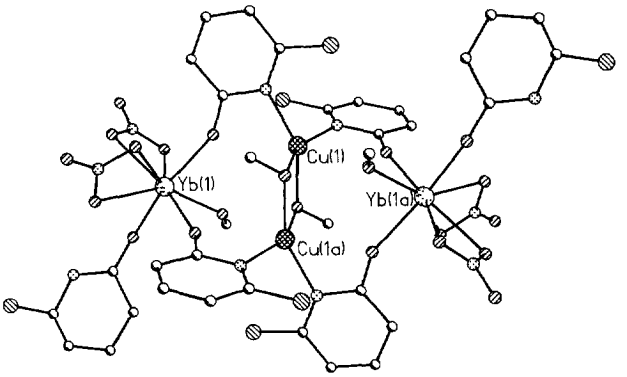

Fig. 34. The structure of $[Cu_2Yb_2(OMe)_2(chp)_4(NO_3)_4(Hchp)_2(MeOH)_2]$ in the crystal (based on data from ref. 162).

discussed above. The synthesis of this complex avoids the use of alcohols, as interference from the formation of methoxide bridges has repeatedly been noticed [6,7,162]. The complex contains eight chp ligands and a further two Hchp units. In this case, the metals are arranged so that the La atoms are at the centre of the molecule, bridged by two μ_2-oxygens from chp ligands (Fig. 35). This compound is the first in which the nitrogen of a pyridone unit is found bound to an f-block element; one of the chp units is η^2 bound to La while the oxygen bridges to one of the copper atoms.

The third complex with a 1:1 ratio of metals has a much more complicated stoichiometry, and a very complicated structure [7]. Four lanthanum atoms form an oxo-bridged plane, which separates two pairs of copper atoms, with the coppers also bridged by oxygen atoms. The structure contains a number of different bridging

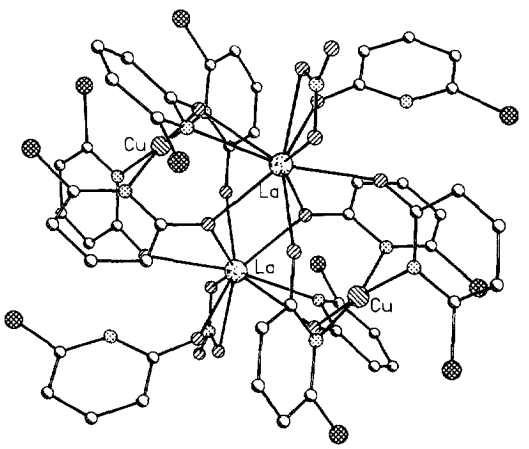

Fig. 35. The structure of $[Cu_2La_2(chp)_8(NO_3)_2(Hchp)_2]$ in the crystal (based on data from ref. 167).

groups, including binucleating and trinucleating hp ligands, methoxide and hydroxide.

The complex with a copper to lanthanum ratio of 3:2 has an extraordinary structure [8]. The metal core consists of $Cu_{12}La_8(OH)_{24}$, surrounded by a sheath of oxygen-bound ligands which include Hmhp, nitrate and water. This sheath of ligands is badly disordered. The metal hydroxide core is far from disordered: the eight La atoms are arranged at the corners of a cube, while the 12 Cu atoms lie at the mid-points of the edges of the cube, forming the cube's edge-double cuboctahedron (Fig. 36). The 24 hydroxides are all bound to two coppers and one lanthanum. Hmhp takes little part in the structure, merely being terminally attached to La atoms. The compound was, however, synthesized via reaction of $[Cu_6Na(mhp)_{12}][NO_3]$ (described in Section 10.1) with hydrated lanthanum nitrate.

The three structurally characterized complexes with a copper to lanthanoid ratio of 2:1 all correspond to a similar type [5,7]. They contain a Cu_4Ln_2 core, which is arranged in a distorted octahedron with the copper atoms in the equatorial plane and the Ln atoms in apical positions (Fig. 37). The metal core is held together by trinucleating hp ligands, which are bound to the oxygen atoms bridging between Cu and Ln, and the nitrogens bound to an additional copper. The Cu atoms in these structures have a square pyramidal coordination geometry, with the equatorial sites occupied by a cis array of two hp nitrogens and two hp oxygens. The apical site is occupied by either chloride, nitrate or water. The lanthanoid ions are either eight or nine coordinate, and again the make-up of the coordination sphere varies between structures. The flexibility of the metal coordination spheres has led to these Cu_4Ln_2 complexes being crystallized as both neutral [5] and charged [7] species.

Three mixed-metal complexes with a copper to metal ratio of 3:1 have been

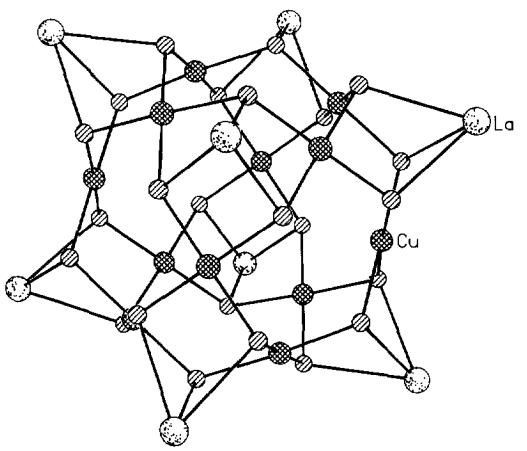

Fig. 36. The $Cu_{12}La_8(OH)_{24}$ core of $[Cu_{12}La_8(OH)_{24}(Hmhp)_{13}(NO_3)_{22}(H_2O)_6][NO_3]_2$ as shown by X-ray crystallography (based on data from ref. 8).

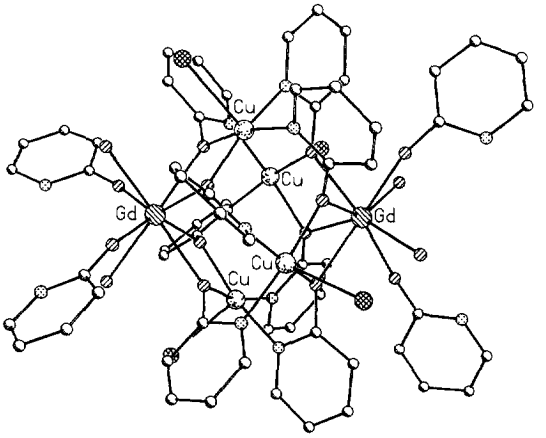

Fig. 37. The structure of the cation $[Cu_4Gd_2(hp)_8(Hhp)_4Cl_4(H_2O)_4]^{2+}$ in the crystal (based on data from ref. 7).

reported. The first is a highly asymmetric complex which contains a Cu_3La core bridged by five chp ligands and one methoxide [167] (Fig. 38). Three of the chp ligands are trinucleating and two binucleating. This complex was synthesized from $[Cu_2(chp)_4]$ (described in Section 10.1), reacted with lanthanum nitrate in methanol. The second complex with this ratio of metals was synthesized in a similar manner, but with the reaction carried out in ethanol [167]. This compound features a Cu_3La core bridged by eight chp ligands (Fig. 39). Here two chp units are trinucleating and five binucleating. The final chp is bound to the La atom via oxygen, and the nitrogen

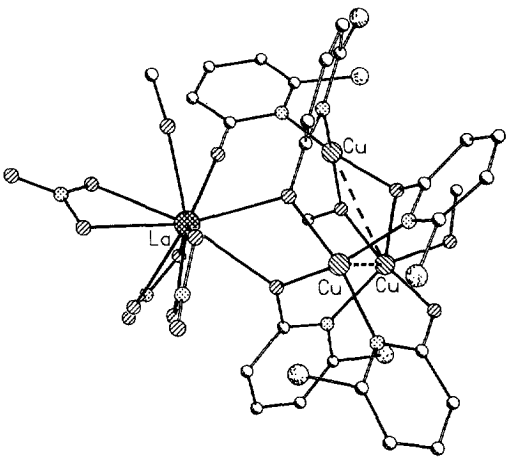

Fig. 38. The structure of $[Cu_3La(chp)_5(OMe)(NO_3)_3(MeOH)_3]$ in the crystal (based on data from ref. 167).

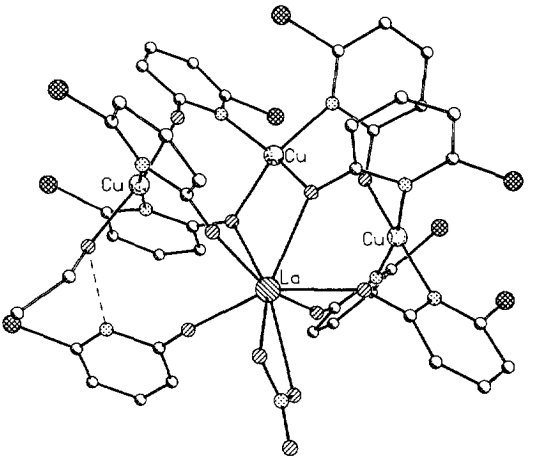

Fig. 39. The structure of $[Cu_3La(chp)_8(NO_3)(EtOH)]$ in the crystal (based on data from ref. 167).

is hydrogen bonded to a molecule of ethanol which is attached to one of the three copper atoms.

A complex with a Cu_3Mg core has also been reported [10]. This was synthesized from the reaction of $[Cu_6Na(mhp)_{12}][NO_3]$ with magnesium nitrate. The structure is similar to that of the second of the Cu_3La complexes discussed above, with Mg replacing La. However, there are only two trinucleating and four binucleating pyridones in the compound, plus two monodentate Hmhp ligands attached to the magnesium.

There are four reported complexes with a copper to metal ratio of 4:1, and they show two structural types. The first type, formed from copper and barium, has a Cu_4Ba core [9], while the second, formed from copper and yttrium or neodymium, has a Cu_8M_2 core [6,164]. The Cu_4Ba complexes feature the Ba atom sandwiched between two pairs of copper atoms — we can imagine the Ba at the centre of a flattened tetrahedron of coppers (Fig. 40). Both complexes contain four hp ligands, bound in a binucleating fashion, with the N atom attached to Cu and the O atom to Ba.

The Cu_8M_2 complexes [166] contain a central portion which corresponds to the metal core of the Cu_4Ln_2 complexes discussed above [5], i.e. four copper atoms in a plane, with two heterometals placed in apical positions to form a distorted octahedron. However, in this case, the "octahedron" contains two μ_4-O atoms, each bound to two coppers and the two apical metals (Fig. 41). All the edges of the octahedron are bridged by μ_2-oxygens from hp ligands, and these hp ligands are bound via their nitrogens to the additional four coppers in the structure. These additional coppers make up two pairs on either side of the central Cu_4M_2 core, with the Cu–Cu vectors perpendicular to the plane of Cu_4 atoms.

Few physical studies have yet been reported for these compounds. Magnetic

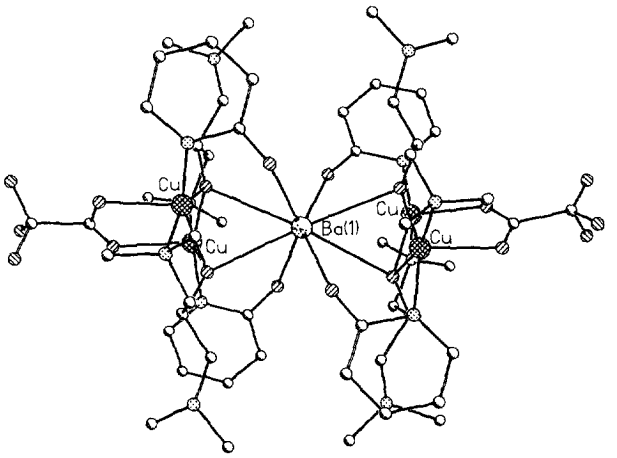

Fig. 40. The structure of $[BaCu_4(hp)_4(bdmap)_4(O_2CCF_3)_2]$ in the crystal (based on data from ref. 9).

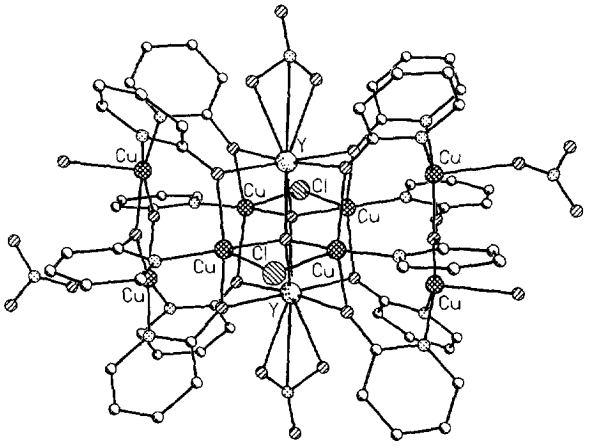

Fig. 41. The structure of $[Cu_8Y_2(O)_2(hp)_{12}Cl_2(NO_3)_4(H_2O)_2]$ in the crystal (based on data from ref. 166).

data have been reported for Cu_4Gd_2 (7), Cu_4La_4 [7], Cu_4Ba [9] and Cu_8Nd_2 [166] complexes. It appears that ferromagnetic coupling occurs between Cu and Gd, concurring with earlier reports based on studies of Schiff base complexes of mixed copper–gadolinium species [168,169]. In all these pyridone compounds, antiferromagnetic coupling is observed between the copper atoms. The compound featuring the anisotropic f-block ion neodymium gave magnetic results which could not be fitted theoretically [166]. Thermal decomposition studies of both Cu_8Y_2 and Cu_8Nd_2 complexes have been reported [166]. Decomposition occurs between 220 and 300°C, with the loss of Hhp being the major process. The resultant phase or phases were not characterized.

11. CONCLUSIONS

11.1. Homometallic dimers with pyridone bridges

One theme which arises from the coordination chemistry of 2-pyridone and its derivatives is the formation of $[M_2(xhp)_4]$ complexes. This work is summarized in Table 9. In addition to the complexes listed, $[Mo_2(php)_4]$ [52], $[Ru_2(bhp)_4]$ [87] and $[Cu_2(3\text{-Ethp})_4(DMF)_2]$ [20] have been reported as C_{2h}, D_{2d} and D_{2d} isomers respectively.

All four possible isomers of the $[M_2(xhp)_4]$ unit have been found. The D_{2d} isomer is the most common, and has been found for 16 combinations of metal and ligand. The C_{4v} isomer occurs chiefly with the fhp ligand, but is also found for chp and hp for Group 8 metals. The C_{2h} and asymmetric 3:1 isomers are each only found in three compounds. For several compounds, e.g. $[Ru_2(chp)_4]$ [87,90] or $[Pd_2(mhp)_4]$ [128,129], more than one isomer has been found. The D_{2d} isomer is clearly the least sterically crowded of the four, but the energy differences between these various isomers have not been studied, nor has the possible interconversion of isomers been reported. For complexes with only two bridging ligands, where there are again four possible isomers (*cis*-HH, *cis*-HT, *trans*-HH and *trans*-HT), NMR studies of complexes of Rh [123] have shown that interconversion of the isomers occurs rapidly at room temperature. This suggests that the energy differences between the isomers are small.

Structural studies on these complexes have been extensive, and have contributed to the understanding of metal–metal bonding. For one series of complexes, the D_{2d} isomers of $[M_2(mhp)_4]$, it is possible to examine the variation in M–M bond length both within a group [1] and across the 4d period. Cotton and co-workers in 1978 showed that, for these compounds, the bond length increases from 1.879(1) Å for M ≡ Cr to 2.161(1) Å for M ≡ W. As the compounds with M ≡ Mo, Ru, Rh and Pd have also been reported, with bond orders varying from four for Mo to zero for Pd, it is also possible to correlate the bond length with the formal bond order. Unfortunately, no complex of Group 7 metals has been reported with the ligand, which makes it difficult to assess the effect of populating the δ^* orbital. However, comparing the Ru, Rh and Pd complexes, the bond length change between Rh and Pd (0.182 Å) is larger than the change between Ru and Rh (0.128 Å). This is consistent with the fact that the σ^* orbital is occupied in the Pd complex, which will have the largest influence on metal–metal bonding.

For Group 6, a large number of physical studies dedicated to the establishment of the nature of the M–M quadruple bond have been reported (see Section 5.3). The number of physical studies diminish rapidly for the remaining compounds. Recent magnetic measurements by Cotton et al. [87,88] on ruthenium dimers indicate that interesting phenomena may also be observed for these complexes.

Compared with physical studies, reactivity studies are much less common for

TABLE 9

Complexes with four bridging pyridone ligands

Metal	$[M_2(hp)_4X_2]$			$[M_2(mhp)_4X]$			$[M_2(chp)_4X]$			$[M_2(fhp)_4X]$		
	Isomer	X	B.L. (Å)	Isomer	X	B.L.[a] (Å)	Isomer	X	B.L.[a] (Å)	Isomer	X	B.L. (Å)
Cr	nr	nr	nr	D_{2d}	None	1.884(5)	D_{2d}	None	1.955(2)	C_{4v}	THF	2.150(2)
Mo	nr	nr	nr	D_{2d}	None	2.065(1)	D_{2d}	None	2.085(1)	C_{4v}	THF	2.092(1)
W	nr	nr	nr	D_{2d}	None	2.161(1)	D_{2d}	None	2.177(1)	C_{4v}	THF	2.185(2)
Tc	[b]	Cl	2.095(2)	nr	nr	nr	nr	nr	nr	nr	nr	nr
Re	C_{2h}	Cl	2.206(2)	nr	nr	nr	nr	nr	nr	nr	nr	nr
Ru	C_{4v}	Cl/Hhp	2.286(1)	D_{2d}	None	2.237(2)	C_{4v}	Cl	2.281(1)	C_{4v}	Cl	2.284(1)
							3:1	Dimer	2.247(1)			
Os	D_{2d}	Cl	2.351(6)	nr	nr	nr	C_{4v}	Cl	2.348(1)	C_{4v}	Cl	2.341(1)
Rh	nr	nr	nr	D_{2d}	None	2.365(6)	D_{2d}	None	2.379(1)	C_{4v}	DMSO	2.410(1)
				3:1	[c]	2.377(8)	3:1	imid	2.385(1)			
Pd	nr	nr	nr	D_{2d}	None	2.547(6)	D_{2d}	None	2.567(4)	nr	nr	nr
				C_{2h}	None	2.559(3)						
Cu	D_{2d}	DMSO	2.587(4)	nr	nr	nr	D_{2d}	None	2.499(1)	nr	nr	nr

[a] Where more than one structure has been reported the average value is given.

[b] Structure is disordered about a crystallographic four-fold axis.

[c] Known with X ≡ Hmhp, imid, CH_3CN and as a dimer.

B.L., bond length; nr, not recorded.

these compounds. Some work has been done on Group 6 [58,68,69] and, recently, work starting from $[Cu_2(chp)_4]$ has been reported [55]. In several cases, higher nuclearity metal complexes result from dimeric precursors [55,70] and therefore it is surprising that so little work has been published.

Despite the extensive work on second- and third-row metals, it is surprising that there is a complete absence of Mn, Fe and Ni complexes of the deprotonated ligand. Given the number of oligomeric Mn and Fe complexes reported for other 1,3-bridging ligands, this is odd. It is suspected that difficulty arises due to the hydrolytic instability of such compounds; however, it seems unlikely that this is an insurmountable obstacle. Moreover, the tendency to form higher oligomers appears greater for the first-row metals and unusual polynuclear complexes might well result.

11.2. Other derivatives

The pyridone derivatives used in the complexes described above are limited. The different reactivity of fhp compared with the other ligands suggests that other structural types may be accessible by the use of further derivatives.

Firstly, the influence of substitution in the 6-position by electronegative groups could be examined by the use of 6-methoxy-2-pyridone or 6-*N*,*N*-dimethylamino-2-pyridone. Also further work should be done on fhp itself, if a suitable synthesis of the ligand can be designed. It is also unclear what effect more extensive substitution of the ring might have on the coordinating ability of the ligands.

Secondly, substitution by bulky groups in the 3-position might affect the binding of the O donor of pyridones. The maximum M–M interaction occurs when the N–M and O–M bonds are essentially parallel. There is a tendency, especially for the heterometallic complexes featuring copper, for the oxygen lone pair to bind anti rather than syn, leading to a much longer M–M contact. Substitution by bulky groups in the 3-position might limit the potential for this to occur. It might also prevent the dimerization of dimers, as observed for some Ru and Rh complexes.

11.3. Future developments

There remains a large amount of unfinished work in this area, e.g. Table 9 shows almost as many gaps as complexes. Additionally, several pieces of work have only begun in the last 5 years or so. For example, the presence of pyridones attached to carbonyl complexes has only been reported in the last 4 years, and then only attached to Ru or Rh complexes [83,84,123,124]. Also the use of pyridones to bridge photoactive centres is a recent development [118–122]. Both of these pieces of work involve mixing a ligand derived from traditional coordination chemistry with organometallic precursors.

Until 1989, the only report of heterometallic complexes of pyridones was that of the mixed Group 6 complexes described by Cotton and Hansen [71]. Since then

two areas of work have arisen. Firstly, the use of pyridone ligands to bridge between copper and "harder" metals [5], e.g. lanthanoids and Group 2 metals, and secondly the use of the php ligand to create mixed molybdenum–palladium arrays [52,72]. This latter piece of work clearly has the potential to be the basis for a great expansion in the number of mixed-metal polynuclear complexes. The ambidentate nature of the pyridone ligand, in itself, suggests this to be a possible area for the future, and synthesizing derivatives with additional donor groups enhances this potential still further.

ACKNOWLEDGEMENTS

We wish to thank the Leverhulme Trust for a post-doctoral fellowship (to J.M.R.) and the Cambridge Crystallographic Database for X-ray data.

REFERENCES

1 F.A. Cotton, P.E. Fanwick, R.H. Niswander and J.C. Sekutowski, J. Am. Chem. Soc., 100 (1978) 4725.
2 F.A. Cotton and J.L. Thompson, J. Am. Chem. Soc., 102 (1980) 6437.
3 J.K. Barton, H.N. Rabinowitz, D.J. Szalda and S.J. Lippard, J. Am. Chem. Soc., 99 (1977) 2827.
4 W. Clegg, C.D. Garner and M.H. Al-Samman, Inorg. Chem., 22 (1983) 1534.
5 D.M.L. Goodgame, D.J. Williams and R.E.P. Winpenny, Polyhedron, 8 (1989) 1531.
6 S. Wang, Inorg. Chem., 30 (1991) 2252.
7 A.J. Blake, P.E.Y. Milne, P. Thornton and R.E.P. Winpenny, Angew. Chem., Int. Ed. Engl., 30 (1991) 1139.
8 A.J. Blake, R.O. Gould, P.E.Y. Milne and R.E.P. Winpenny, J. Chem. Soc., Chem. Commun., (1991) 1453.
9 S. Wang, S.J. Trepanier and M.J. Wagner, Inorg. Chem., 32 (1993) 833.
10 A.J. Blake, R.O. Gould, C.M. Grant, P.E.Y. Milne, D. Reed and R.E.P. Winpenny, Angew. Chem., Int. Ed. Engl., 33 (1994) 195.
11 S.J. Lippard, Angew. Chem., Int. Ed. Engl., 27 (1988) 353, and references cited therein.
12 S.L. Heath and A.K. Powell, Angew. Chem., Int. Ed. Engl., 31 (1992) 191.
13 G. Christou, Acc. Chem. Res., 22 (1989) 328, and references cited therein.
14 E. Libby, J.K. McCusker, E.A. Schmitt, K. Folting, D.N. Hendrickson and G. Christou, Inorg. Chem., 30 (1991) 3486.
15 G.R. Newkom, J. Broussard, S.K. Staines and J.D. Sauer, Synthesis, (1974) 707.
16 O.A. Zeide and A.T. Titov, Berichte, 69B (1936) 1884.
17 O. Seide, Berichte, 57 (1924) 793, 1805.
18 C.J. Donahue, V.A. Martin, B.A. Schoenfelner and E. Kosinski, Inorg. Chem., 30 (1991) 1588.
19 G.R. Newkom and D.C. Hager, J. Org. Chem., 43 (1978) 947.
20 Y. Nishida and S. Kida, Bull. Chem. Soc. Jpn., 58 (1985) 383.
21 S. Emori, R. Furakuwa and S. Nakushima, Bull. Chem. Soc. Jpn., 63 (1990) 2426.
22 S. Emori, H. Suenaga and N. Goto, Bull. Chem. Soc. Jpn., 64 (1991) 3460.
23 W.P. Griffith and S.L. Mostafa, Polyhedron, 11 (1992) 2997.

24 F. Baker and E.C.C. Baly, J. Chem. Soc., 91 (1907) 1122.
25 A.R. Katritzky and J.M. Lagowski, Adv. Heterocycl. Chem., 1 (1963) 312.
26 J. Elguero, C. Marzin, A.R. Katritzky and P. Linda, Adv. Heterocycl. Chem., S1 (1976) 1.
27 M.W. Wong, K.B. Wiberg and M.J. Frisch, J. Am. Chem. Soc., 114 (1992) 1645, and references cited therein.
28 O.G. Parchment, I.H. Hillier and D.V.S. Green, J. Chem. Soc., Perkin Trans. II, (1991) 799.
29 P. Beak, F.S. Fry, J. Lee and F. Steele, J. Am. Chem. Soc., 98 (1976) 171.
30 B.R. Penfold, Acta Crystallogr., 6 (1953) 591.
31 A. Kvick, Acta Crystallogr., Sect. B, 32 (1976) 220.
32 A. Kvick and I. Olovsson, Ark. Khim., 30 (1968) 71.
33 A. Kvick and S.S. Booles, Acta Crystallogr., Sect. B, 28 (1972) 3405.
34 J. Almlof, A. Kvick and I. Olovsson, Acta Crystallogr., Sec. B, 27 (1971) 1201.
35 D. Taylor, Aust. J. Chem., 28 (1975) 2615.
36 D.M.L. Goodgame, D.J. Williams and R.E.P. Winpenny, Inorg. Chim. Acta, 166 (1989) 159.
37 A.J. Blake, R.O. Gould, C.M. Grant, P.E.Y. Milne and R.E.P. Winpenny, Polyhedron, 13 (1994) 187.
38 L.S. Hollis and S.J. Lippard, Inorg. Chem., 22 (1983) 2708.
39 E. Spinner and J.C.B. White, J. Chem. Soc. (B), (1966) 991.
40 M. Kuzuya, A. Noguchi and T. Okuda, J. Chem. Soc., Perkin Trans. II, (1985) 1423.
41 D.G. de Kowalewski, R.H. Contreras and C. de los Santos, J. Mol. Struct., 213 (1989) 201.
42 D.W. Boykin, D.W. Sullins, N. Pourahmady and E.J. Eisenbraun, Heterocycles, 29 (1989) 307.
43 E.S. Gould, J. Am. Chem. Soc., 89 (1967) 5792.
44 E.S. Gould, J. Am. Chem. Soc., 90 (1968) 1740.
45 J. Reedijk, Recl. Trav. Chim., 88 (1969) 1139.
46 J. Reedijk, Recl. Trav. Chim., 91 (1972) 681.
47 A.G. Orpen, L. Brammer, F.H. Allen, O. Kennard, D.G. Watson and R. Taylor, J. Chem. Soc., Dalton Trans., (1989) S1.
48 D.M.L. Goodgame, S. Newnham, C.A. O'Mahoney and D.J. Williams, Polyhedron, 9 (1990) 491.
49 F.A. Cotton, G.E. Lewis and G.N. Mott, Inorg. Chem., 22 (1983) 378.
50 F.A. Cotton, W.H. Ilsley and W. Kaim, Inorg. Chem., 19 (1980) 1453.
51 F.A. Cotton, L.R. Falvello, S. Han and W. Wang, Inorg. Chem., 22 (1983) 4106.
52 K. Mashima, H. Nakano, T. Mori, H. Takaya and A. Nakamura, Chem. Lett., (1992) 185.
53 P.E. Fanwick, B.E. Bursten and G.B. Kaufmann, Inorg. Chem., 24 (1985) 1165.
54 M.H. Al-Samman, M.Sc. Thesis, University of Manchester, cited in ref. 66.
55 A.J. Blake, C.M. Grant, P.E.Y. Milne, J.M. Rawson and R.E.P. Winpenny, J. Chem. Soc., Chem. Commun., (1994) 169.
56 M.K. Chisholm, K. Folting, J.C. Huffman and I.P. Rothwell, Inorg. Chem., 20 (1981) 1854.
57 M.K. Chisholm, K. Folting, J.C. Huffman and I.P. Rothwell, Inorg. Chem., 20 (1981) 2215.
58 P.E. Fanwick, Inorg. Chem., 24 (1985) 258.
59 M.J. Calhorda, M.A.A.F. De C.T. Carrondo, R.G. Da Costa, A.R. Dias, M.T.L.S. Duarte and M.B. Hursthouse, J. Organomet. Chem., 320 (1987) 53.
60 A. Mitschler, B. Rees, R. Wiest and M. Benard, J. Am. Chem. Soc., 104 (1982) 7501.
61 W. Clegg, C.D. Garner, L. Akhter and M.H. Al-Samman, Inorg. Chem., 22 (1983) 2466.
62 M.C. Manning and W.C. Trogler, J. Am. Chem. Soc., 105 (1983) 5311.
63 C.D. Garner, I.H. Hillier, A.A. MacDowell, I.B. Walton and M.F. Guest, J. Chem. Soc., Faraday Trans. II, 75 (1979) 485.

64 C.D. Garner, I.H. Hillier, M.J. Knight, A.A. MacDowell, I.B. Walton and M.F. Guest, J. Chem. Soc., Faraday Trans. II, 76 (1980) 885.
65 B.E. Bursten, F.A. Cotton, A.H. Cowley, B.E. Hanson, M. Lattman and G.E. Stanley, J. Am. Chem. Soc., 101 (1979) 6244.
66 M. Berry, C.D. Garner, I.H. Hillier, A.A. MacDowell, and I.B. Walton, Chem. Phys. Lett., 70 (1980) 350.
67 K.J. Cavell, C.D. Garner, J.A. Martinho-Simoes, G. Pilcher, H. Al-Samman, H.A. Skinner, G. Al-Tekhin, I.B. Walton and M.T. Zafarani-Moattar, J. Chem. Soc., Faraday Trans. I, 77 (1981) 2927.
68 D. DeMarco, T. Nimry and R.A. Walton, Inorg. Chem., 19 (1980) 575.
69 F.A. Cotton, R.H. Niswander and J.C. Sekutowski, Inorg. Chem., 17 (1978) 3541.
70 L. Akhter, W. Clegg, D. Collison and C.D. Garner, Inorg. Chem., 24 (1985) 1725.
71 F.A. Cotton and B.E. Hanson, Inorg. Chem., 17 (1978) 3237.
72 K. Mashima, H. Nakano and A. Nakumura, J. Am. Chem. Soc., 115 (1993) 11 632.
73 D.P. Kessissoglou, M.L. Kirk, C.A. Bender, M.S. Lah and V.L. Pecoraro, J. Chem. Soc., Chem. Commun., (1989) 84.
74 F.A. Cotton, P.E. Fanwick and L.D. Gage, J. Am. Chem. Soc., 102 (1980) 1570.
75 A.R. Cutler, S.M.V. Esjornson, P.E. Fanwick and R.A. Walton, Inorg. Chem., 27 (1988) 287.
76 F.A. Cotton and L.D. Gage, Inorg. Chem., 18 (1979) 1716.
77 A.R. Cutler and R.A. Walton, Inorg. Chim. Acta, 105 (1985) 219.
78 F.A. Cotton and T. Ren, Polyhedron, 11 (1992) 811.
79 P.E. Fanwick, M. Leeaphon and R.A. Walton, Inorg. Chem., 29 (1990) 676.
80 M. Leeaphon, P.E. Fanwick and R.A. Walton, Inorg. Chem., 30 (1991) 4986.
81 F.A. Cotton and J.L. Thompson, Inorg. Chim. Acta, 44 (1980) L247.
82 F.A. Cotton, K.R. Dunbar and M. Matusz, Inorg. Chem., 25 (1986) 1585.
83 P.L. Andreu, J.A. Cabeza, G.A. Carriedo, V. Riera, S. Garcia-Granda, J.F. Van der Maelen and G. Mori, J. Organomet. Chem., 421 (1991) 305.
84 S.J. Sherlock, M. Cowie, E. Singleton and M.M. de V. Steyn, J. Organomet. Chem., 361 (1989) 353.
85 M. Berry, C.D. Garner, I.H. Hillier and W. Clegg, Inorg. Chim. Acta, 53 (1981) L61.
86 W. Clegg, Acta Crystallogr., Sect. B, 36 (1980) 3112.
87 F.A. Cotton, T. Ren and J.L. Eglin, J. Am. Chem. Soc., 112 (1990) 3439.
88 F.A. Cotton, T. Ren and J.L. Eglin, Inorg. Chem., 30 (1991) 2552.
89 A.R. Chakravarty, F.A. Cotton and D.A. Tocher, Inorg. Chem., 24 (1985) 172.
90 A.R. Chakravarty, F.A. Cotton and D.A. Tocher, Inorg. Chem., 24 (1985) 1263.
91 A.R. Chakravarty, F.A. Cotton and W. Schwotzer, Polyhedron, 5 (1986) 1821.
92 A.R. Chakravarty, F.A. Cotton and D.A. Tocher, Inorg. Chem., 24 (1985) 2857.
93 A.R. Chakravarty and F.A. Cotton, Inorg. Chim. Acta, 105 (1985) 19.
94 F.A. Cotton and M. Matusz, Polyhedron, 6 (1987) 1439.
95 F.A. Cotton, K.R. Dunbar and M. Matusz, Inorg. Chem., 25 (1986) 1589.
96 A.J. Lindsay, G. Wilkinson, M. Motevalli and M.B. Hursthouse, J. Chem. Soc., Dalton Trans., (1985) 2321.
97 J.G. Norman, G.E. Renzoni and D.A. Case, J. Am. Chem. Soc., 101 (1979) 5236.
98 T. Behling, G. Wilkinson, T.A. Stephenson, D.A. Tocher and M.D. Walkinshaw, J. Chem. Soc., Dalton Trans., (1983) 2109.
99 T.W. Johnson, S.M. Tetrick and R.A. Walton, Inorg. Chim. Acta, 167 (1990) 133.
100 S.M. Tetrick, V.T. Coombe, G.A. Heath, T.A. Stephenson and R.A. Walton, Inorg. Chem., 23 (1984) 4567.

101 W. Clegg, M. Berry and C.D. Garner, Acta Crystallogr., Sect. B, 36 (1980) 3110.
102 E.C. Morrison, C.A. Palmer and D.A. Tocher, J. Organomet. Chem., 349 (1988) 405.
103 P. Lauhuerta, J. Latorre, M. Sanau, F.A. Cotton and W. Schwotzer, Polyhedron, 7 (1988) 1311.
104 N. Lugan, F. Laurent, G. Lavigne, T.P. Newcombe, E.W. Limatta and J.-J. Bonnet, Organometallics, 11 (1992) 1351.
105 M. Berry, C.D. Garner, I.H. Hillier, A.A. MacDowell and W. Clegg, J. Chem. Soc., Chem. Commun., (1980) 494.
106 W. Clegg, Acta Crystallogr., Sect. B, 36 (1980) 2437.
107 W. Clegg, C.D. Garner, L. Akhter and M.H. Al-Samman, Inorg. Chem., 22 (1983) 2466.
108 F.A. Cotton and T.R. Felthouse, Inorg. Chem., 20 (1981) 584.
109 F.A. Cotton, S. Han and W. Wang, Inorg. Chem., 23 (1984) 4762.
110 M. Berry, C.D. Garner, I.H. Hillier and W. Clegg, Inorg. Chim. Acta, 45 (1980) L209.
111 W. Clegg, L. Akhter and C.D. Garner, J. Chem. Soc., Chem. Commun., (1984) 101.
112 F.A. Cotton and S.-J. Kang, Inorg. Chim. Acta, 209 (1993) 23.
113 F.A. Cotton and R.A. Walton, Multiple Bonds Between Metal Atoms, Wiley, New York, 2nd edn., 1993.
114 C.D. Garner, M. Berry and B.E. Mann, Inorg. Chem., 23 (1984) 1500.
115 D.A. Tocher and J.H. Tocher, Inorg. Chim. Acta, 131 (1987) 69.
116 V. Gutmann, Electrochim. Acta, 21 (1976) 661.
117 R.S. Drago, S.P. Tanner, R.M. Richman and J.R. Long, J. Am. Chem. Soc., 101 (1979) 2897.
118 G.S. Rodman and K.R. Mann, Inorg. Chem., 24 (1985) 3507.
119 G.S. Rodman and K.R. Mann, Inorg. Chem., 27 (1988) 3338.
120 G.S. Rodman, C.A. Daws and K.R. Mann, Inorg. Chem., 27 (1988) 3347.
121 D.C. Boyd, R. Szalapski and K.R. Mann, Organometallics, 8 (1989) 790.
122 T. Sielisch and M. Cowie, Organometallics, 7 (1988) 707.
123 M.A. Ciriano, B.E. Villarroya, L.A. Oro, M.C. Apreda, C. Foces-Foces and F.H. Cano, J. Organomet. Chem., 366 (1989) 377.
124 M.A. Ciriano, B.E. Villarroya, L.A. Oro, M.C. Apreda, C. Foces-Foces and F.H. Cano, J. Chem. Soc., Dalton Trans., (1987) 981.
125 J.L. Herde, J.C. Lambert and C.V. Senoff, Inorg. Synth., 15 (1974) 18.
126 K.A. Beveridge, G.W. Bushnell, S.R. Stobart, J.L. Atwood and M.J. Zaworothko, Organometallics, 2 (1983) 1447.
127 J.V. Caspar and H.B. Gray, J. Am. Chem. Soc., 106 (1984) 3029.
128 W. Clegg, C.D. Garner and M.H. Al-Samman, Inorg. Chem., 21 (1982) 1897.
129 D.P. Bancroft, F.A. Cotton, L.R. Falvello and W. Schwotzer, Inorg. Chem., 25 (1986) 1015.
130 J.K. Barton, D.J. Szalda, H.N. Rabinowitz, J.V. Waszczak and S.J. Lippard, J. Am. Chem. Soc., 101 (1979) 1434.
131 L.S. Hollis and S.J. Lippard, J. Am. Chem. Soc., 103 (1981) 1230.
132 L.S. Hollis and S.J. Lippard, J. Am. Chem. Soc., 103 (1981) 6761.
133 L.S. Hollis and S.J. Lippard, Inorg. Chem., 22 (1983) 2116.
134 L.S. Hollis and S.J. Lippard, Inorg. Chem., 22 (1983) 2600.
135 L.S. Hollis and S.J. Lippard, Inorg. Chem., 22 (1983) 2605.
136 L.S. Hollis, M.M. Roberts and S.J. Lippard, Inorg. Chem., 22 (1983) 3637.
137 L.S. Hollis and S.J. Lippard, J. Am. Chem. Soc., 105 (1983) 3494.
138 T.V. O'Halloran, M.M. Roberts and S.J. Lippard, J. Am. Chem. Soc., 106 (1984) 6427.
139 T.V. O'Halloran, M.M. Roberts and S.J. Lippard, Inorg. Chem., 25 (1986) 957.
140 T.V. O'Halloran, P.K. Mascharak, I.D. Williams, M.M. Roberts and S.J. Lippard, Inorg. Chem., 26 (1987) 1261.

141 D.P. Bancroft, F.A. Cotton, L.R. Falvello and W. Schwotzer, Inorg. Chem., 25 (1986) 763.
142 D.P. Bancroft and F.A. Cotton, Inorg. Chem., 27 (1988) 1633.
143 D.P. Bancroft and F.A. Cotton, Inorg. Chem., 27 (1988) 4022.
144 K. Suzuki and K. Matsumoto, Chem. Lett., (1989) 317.
145 K. Matsumato, H. Moriyama and K. Suzuki, Inorg. Chem., 29 (1990) 2096.
146 M. Goodgame and D.J. Jakubovic, Coord. Chem. Rev., 79 (1987) 97, and references cited therein.
147 J.K. Barton, C. Caravana and S.J. Lippard, J. Am. Chem. Soc., 101 (1979) 7269.
148 B.K. Teo, K. Kijima and R. Bau, J. Am. Chem. Soc., 100 (1978) 621.
149 J.K. Barton, S.A. Best, S.J. Lippard and R.A. Walton, J. Am. Chem. Soc., 100 (1978) 3785.
150 K. Matsumato, H. Takahashi and K. Fuwa, Inorg. Chem., 22 (1983) 4086.
151 P.K. Mascharak, I.D. Williams and S.J. Lippard, J. Am. Chem. Soc., 106 (1984) 6428.
152 A.P. Ginsberg, T.V. O'Halloran, P.E. Fanwick, L.S. Hollis and S.J. Lippard, J. Am. Chem. Soc., 106 (1984) 5430.
153 A.J. Blake, R.O. Gould and R.E.P. Winpenny, Acta Crystallogr., Sect. C, 47 (1991) 1077.
154 A.J. Blake and R.E.P. Winpenny, Acta Crystallogr., Sect. C, 49 (1993) 799.
155 S.K. Yeh, D.S. Liaw and S.M. Peng, Bull. Inst. Chem., Acad. Sin., 34 (1987) 49.
156 S. Emori, I. Okano and Y. Muto, Bull. Chem. Soc. Jpn., 45 (1972) 3717.
157 B. Bleaney and K.D. Bowers, Proc. R. Soc. London, Ser. A, 214 (1952) 451.
158 D.M.L. Goodgame, Y. Nishida and R.E.P. Winpenny, Bull. Chem. Soc. Jpn., 59 (1986) 344.
159 J. Catterick and P. Thornton, Adv. Inorg. Radiochem., 20 (1977) 291.
160 A. Terzis, A.N. Beauchamp and R. Rivest, Inorg. Chem., 12 (1973) 1166.
161 Y. Nishida, M. Matsumato and Y. Mori, Z. Naturforsch., Teil B, 44 (1989) 307.
162 A.J. Blake, R.O. Gould, P.E.Y. Milne and R.E.P. Winpenny, J. Chem. Soc., Chem. Commun., (1992) 522.
163 M. Berry, W. Clegg, C.D. Garner and I.H. Hillier, Inorg. Chem., 21 (1982) 1342.
164 F. Bonati, A. Burini, B.R. Pietroni and B. Bovio, J. Organomet. Chem., 296 (1985) 301.
165 G. Bednorz and K.A. Müller, Z. Phys. B, 64 (1986) 189.
166 S. Wang, Z. Pang and M.J. Wagner, Inorg. Chem., 31 (1992) 5381.
167 A.J. Blake, P.E.Y. Milne and R.E.P. Winpenny, J. Chem. Soc., Dalton Trans., (1993) 3727.
168 A. Bencini, C. Benelli, A. Caneschi, A. Dei and D. Gatteschi, J. Am. Chem. Soc., 107 (1985) 8128.
169 N. Matsumato, M. Sakamoto, H. Tamaki, H. Okawa and S. Kida, Chem. Lett., (1989) 853.